AD-A147 212 INTERMEDIATE RESULTS OF RADAR BACKSCATTER MEASUREMENTS FROM SUMMER SEA IC.. (U) KANSAS UNIV/CENTER FOR RESEARCH INC LAWRENCE REMOTE SENSING L.. S GOGINENI ET AL. 1/1

UNCLASSIFIED JUL 84 RSL-TR-3311-2 N00014-76-C-1105 F/G 20/14 NL

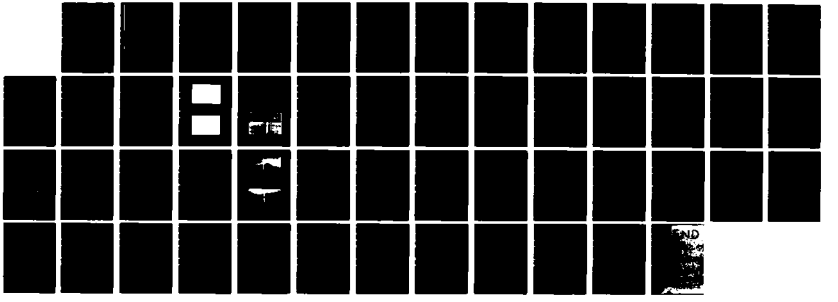

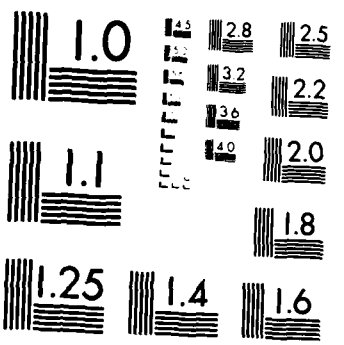

REMOTE SENSING LABORATORY

INTERMEDIATE RESULTS OF RADAR BACKSCATTER MEASUREMENTS FROM SUMMER SEA ICE

THE UNIVERSITY of KANSAS CENTER for RESEARCH, INC.

2291 Irving Hill Drive-Campus West

Lawrence, Kansas 66045

INTERMEDIATE RESULTS OF RADAR BACKSCATTER MEASUREMENTS FROM SUMMER SEA ICE

S. Gogineni
R.G. Onstott
R.K. Moore
J. Chancellor

Remote Sensing Laboratory
University of Kansas
Center for Research, Inc.
Lawrence, Kansas 66045-2969

RSL Technical Report
RSL TR 3311-2

July 1984

Supported by:

OFFICE OF NAVAL RESEARCH
Department of the Navy
800 N. Quincy Street
Arlington, Virginia 22217

Contract N00014-76-C-1105

TABLE OF CONTENTS

letter on file

A-1

LIST OF FIGURES

LIST OF TABLES

ABSTRACT

The helicopter-borne scatterometer (HELOSCAT) was used to measure radar backscatter from sea ice under summer conditions near Mould Bay, N.W.T., Canada, in June and July 1982. These measurements were made at selected frequencies between 1 and 17 GHz, and at angles between 5° and 60° with like- and cross-polarizations.

Multiyear ice (MYI) can be distinguished from first-year ice (FYI) using the profiles acquired by flying the helicopter along selected scan lines at 5.2, 9.6 and 13.6 GHz during early and late summer.

Because of wet snow and ice on the surface, producing reduced volume scatter, there is lower backscatter from MYI during summer than during winter. Because of superimposed ice, the backscatter from FYI during early summer is slightly higher than that during other seasons Its backscatter is higher than that of MYI for the early part of summer, but as summer progresses, FYI backscatter reduces and eventually becomes lower than that from MYI.

The results indicate that higher frequencies in Ku- and X-bands are not better than lower frequencies in C-band for discriminating basic ice types during summer. The backscatter from MYI and FYI increased with frequency, and the contrast between FYI and MYI increased with decreasing frequency during late summer.

1.0 INTRODUCTION

A large portion of the ocean (approximately 10% - 13%) is covered with ice. Because it is reported that these regions have a significant impact on global weather and that Arctic and Antarctic regions are rich in mineral and natural resources, long-term ice monitoring on a global scale is necessary to understand the interaction between ocean, ice and atmosphere and solve the operational problems associated with resources exploitation [Weeks, 1981]. The "class of ship or ice breaker" needed for safe and economical navigation through ice-infested waters is determined by the age or thickness of the ice [Luther et al., 1982]. Operational problems associated with oil and natural gas exploration in the Arctic involve not only designing systems that can survive the harsh Arctic environment, but also require the prediction of possible collision of pack ice with a drilling ship or platform.

Remote sensing devices operating in the visible or infrared spectrum have limited use in global ice monitoring since areas covered with sea ice are shrouded in darkness or cloud cover a significant part of the year [Weeks, 1981]. Therefore, weather-independent microwave remote sensing systems operating in the 1 - 30 cm wavelength region are needed to provide year-round coverage as well as supplement the data available from other sensors.

Passive microwave systems for sea ice study have received more attention than active microwave systems. The reason is the availability of spaceborne systems, some of which are still operational [Weeks, 1981; Gloersen et al., 1983]. The resolution of spaceborne passive systems is poor. Resolution between 2 and 50 km may be adequate for monitoring some sea ice parameters such as concentration and type, but resolution between 10 and 100 m is required for monitoring some other parameters such as ridging and opening and closing of leads. The spaceborne microwave remote sensing system with the

greatest potential for ice study is synthetic-aperture radar (SAR). Several studies conducted with airborne SAR systems have proven that several ice parameters (extent, types, concentration, drift and ridges) can be extracted from SAR images or from a combination of SAR images and information from other sensors [Luther et al., 1982; Livingstone et al., 1980].

A major disadvantage of spaceborne SAR is high data flow rate [Luther et al., 1982]. Some of the operations associated with natural resource exploitation in areas covered with sea ice require near-real-time ice forecasting. The processing and analysis of SAR images needs to be automated for real-time ice forecasting. This requires development of intelligent algorithms to extract the maximum information from SAR images. Radar return from sea ice depends on its electrical (dielectric constant) and physical properties (surface roughness, volumetric structure), and systemm parameters (frequency, polarization and incidence angle). The optimum radar parameters can be selected only by understanding interaction between electromagnetic waves and sea ice. This necessitates the measurement of backscatter from sea ice during different seasons and at various locations, and subsequent development of theoretical models to explain the backscatter mechanism.

A large number of radar backscatter experiments have been conducted with airborne and surface-based systems during the last few years. These experiments, except those by Onstott et al. [1980] and Gray et al. [1982] were conducted during winter. The experiment by Gray et al. [1982] was conducted during late summer. The experiment by Onstott et al. [1980] was restricted to frequencies between 8 and 17 GHz.

The University of Kansas collected radar backscatter from sea ice during June - July 1982 to supplement the existing data base and extend the measurements to the early part of summer and to lower frequencies in C- and L-

bands. Coincident passive microwave measurements and detailed surface observations were also made during this experiment.

The purpose of this report is to summarize the data collected during June - July 1982 summer experiment from ice located near Mould Bay, N.W.T., Canada. A brief description of the system used for data acquisition and experiment are given in Sections 2.0 and 3.0, respectively. Time histories are shown in Section 4.0; angular and frequency responses of multiyear and first-year ice are in Section 5.0; Section 6.0 shows comparison of backscatter from different sites; and comparison of the backscatter from sea ice during fall and summer conditions are in Section 7.0. Conclusions and future experiment recommendations are given in Section 8.0.

2.0 SYSTEM DESCRIPTION

The University of Kansas helicopter-borne spectrometer (HELOSCAT III), which was operated from a Bell 206 helicopter, made backscatter measurements of sea ice at frequencies between 1 and 17 GHz, incidence angles between 5° - 70° with like- and cross-antenna polarizations. The system specifications are given in Table 1.

Relative calibration of the system was performed by measuring the signal from a delay line of known loss. Absolute calibration was obtained by measuring power received from a target of known radar cross section. A more detailed description of the system is available in Gogineni et al. [1984].

TABLE 1
NOMINAL SYSTEM SPECIFICATIONS

	X-Ku-Band	L-Band
Type	FM-CW	FM-CW
Frequency Range	4-18 GHz	1-2 GHz
Modulation	Triangular	Triangular
Sweep Bandwidth	750 MHz	800 MHz
Transmitter Power	10-19 dBm	19 dBm
IF Frequency	50 kHz	50 kHz
IF Bandwidth	13.5 kHz	13.5 kHz
Antennas:	Parabolic Reflectors with Log-Periodic Feeds	
Polarization	VV	
Size	46 cm	
Beamwidths	6.4, 4.4, 3.8 and 3.4 at 4.8, 7.2, 9.6 and 13.6 GHz	
Polarization	HH	HH
Size	61 cm	46 and 61 cm
Beamwidths	5.0, 3.4, 2.5 and 1.9 at 4.8, 7.2, 9.6 and 13.6 GHz	11.4
Polarization	HV	
Size	46 cm and 61 cm	
Beamwidths	5.6, 3.8, 3.4 and 2.6 at 4.8, 7.2, 9.6 and 13.6 GHz	
Incidence Angles	5° - 70°	5° - 70°
Calibration:		
Relative	Delay line	Delay line
Absolute	Luneberg lens	Corner reflector
Altitude	30 m for θ = 5 to 21 15 m for θ > 30	30 m for θ = 5 to 21 15 m for θ > 30

3.0 EXPERIMENT AND SITE DESCRIPTION

3.1 Experiment Description

Measurements of radar backscatter from sea ice under summer conditions (June - July 1982) were made as part of the RADARSAT/FIREX program. The high Arctic weather station operated by AES, Canada, and located at Mould Bay, N.W.T., served as the base camp. Backscatter measurements in conjunction with

detailed surface observations were made on four sites near Mould Bay. A map of Mould Bay and the surroundings is shown in Figure 3.1.

Flight lines were established by careful survey of the site by the scientific team and markers to encode different ice conditions in the data stream are placed along the flight path. The primary emphasis in data collection was to acquire full-length profiles of the site at 5.2, 9.6 and 13.6

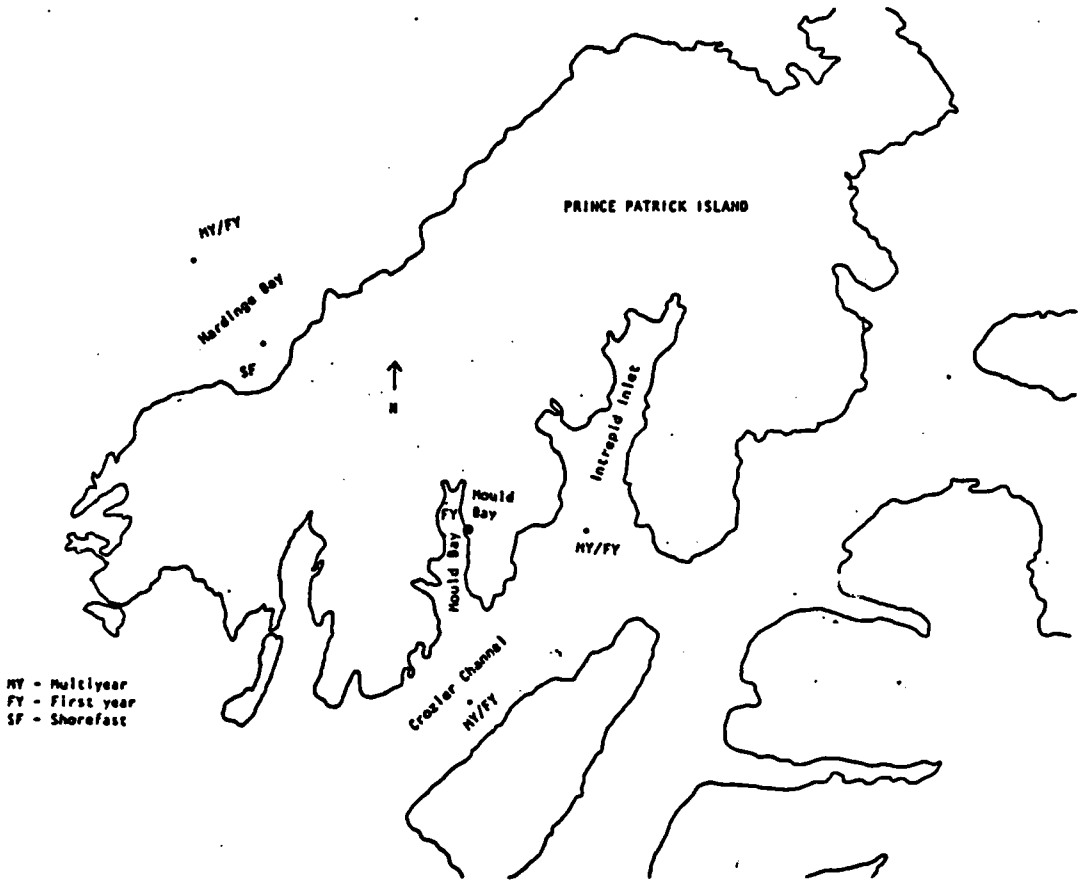

FIGURE 3.1: Map of Mould Bay and Surrounding Area with 1982 Ice Sites

GHz with HH-polarization. The measurements were extended as much as possible to other frequencies and polarizations. Basically, two types of ice were investigated during this experiment: first-year (FYI) and multiyear (MYI).

In addition, features such as pressure ridges (PR) and meltpools (MP) were studied.

Small-scale surface roughness measurements were also made by physically removing long sections of ice. Thin sections of ice were cut from these long sections and photographed against a centimeter grid. These data are not included in this report, but will be discussed in individual reports at a later time.

3.2 Site Descriptions

During backscatter measurements, ice characterization measurements were made along the HELOSCAT flight line. Ice cores were collected for chemical analysis. Line surveys were made to describe qualitatively the surface characteristics along the line, and measurements were taken to describe snow and ice thickness and general condition of ice and snow. Photographs were taken to provide permanent records to support qualitative descriptions of the site. Long ice blocks were cut and transported to the base camp for small-scale roughness measurement. A brief summary of the sites' physical description is provided below.

3.2.1 Mould Bay

The thick first-year ice in Mould Bay was approximately 2.4 m thick. During the beginning of this investigation (near pre-melt conditions) the ice surface was covered with a humid snow cover. The average depth of snow cover on this site is given in Table 2. Refreezing of free water which percolates through the snowpack on the sea ice surface causes the formation of superimposed ice. The snow cover melted rapidly and by June 24 there was over 50% puddling and by June 25 there was 90% puddling. The maximum depth of water

was about 5 cm [Digby, 1982]. Some draining occurred through the breathing holes of seals and tension cracks. By June 29, the ice was saturated with water and a few drained areas were visible.

TABLE 2
SNOW DEPTH ON MOULD BAY

Snow depth (cm)

Date	Site Marker							
	0	1	2	3	4	5	6A	7
6/13			14.5	16.0		9.5		15.0
6/16		9.8						14.5
6/17				10.0				9.0
6/21		2-4	11.5	6.6	5-8	18-39 (drift)	1.5-4.5	
6/22				3.5				
6/24	Flooded snow cover							
6/29	Over 80% of the surface is covered with water							

3.2.2 Peach Pit

This site, located in Crozier Channel, was a multiyear floe frozen in first-year ice. The surface of the first-year ice near station 0 was gently undulating with a small-scale roughness of less than 1 cm superimposed on the undulations. The peaks of the undulations were between 4 and 5 cm. The surface of the ice had varying degrees of roughness between stations 0 and 1. It was smooth at a few places and slightly rough at some other places.

The average depth of the snow cover was about 4 cm. A snow drift as large as 1 m deep, approximately 210 m from marker 1, was observed on the left-hand side of the flight line. The snow was wet and granular with ice

crystals as large as 1-2 cm. The snow surface was slightly rough in some places and moderately rough in other places, as shown in Figures 3.2 and 3.3.

The MYI surface undulated with up to 1 m peaks. The surface of the ice on hummocks was wet and generally smooth. Snow cover on the hummocks was less than 2 cm. The depth of snow on the sides of meltpools was between 10 and 20 cm. The large-scale roughness of multiyear ice caused snow drifts and hollows, as shown in Figure 3.4. Snow on MYI was soft, wet and fine-grained. The snow surface on MYI was also smoother than that on FYI.

The depth of water on June 22 in the meltpools was between 5 and 20 cm. Ice at the bottom of the ponds was generally very smooth. By evening and during mornings, many meltpools were topped with a thin layer of ice.

The surface of FYI was covered with water by June 29, as shown in Figure 3.5. This water drained through seals' breathing holes and tension cracks and some drained areas were visible on July 2. The size ofthe meltpools on the MYI had increased in many places.

3.2.3 Intrepid

This was a site of heavily weathered MYI frozen in the FYI of Intrepid Inlet. Most of the multiyear floe had rounded peaks except for rubble near station 0. A large 6 m high weathered pressure ridge intersected the flight line approximately 1/3 of the way through the MY floe. The ice on the ridge was smooth and had a 2-5 cm snow cover. The depth of snow cover in the valleys of the ridge ranged from 20 to 60 cm. The ice on the hummocks was generally smooth with a wet snow cover 1-6 cm thick. A rubble field near station 0 contained large 1-m ice blocks. The smooth surfaces of these ice blocks were covered with 1-3 cm wet snow cover. Voids between the ice blocks were filled with wet snow.

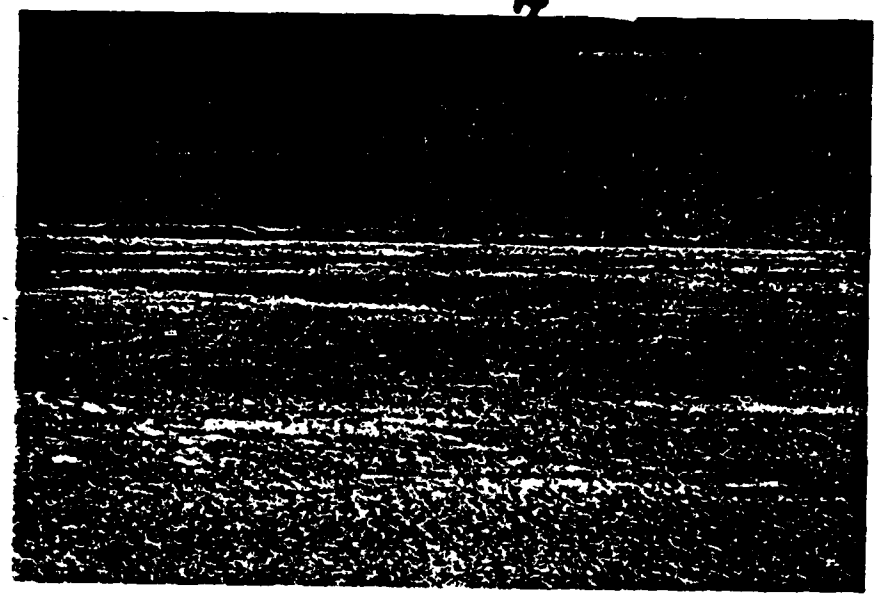

FIGURE 3.2
Slightly Rough Snow on FYI

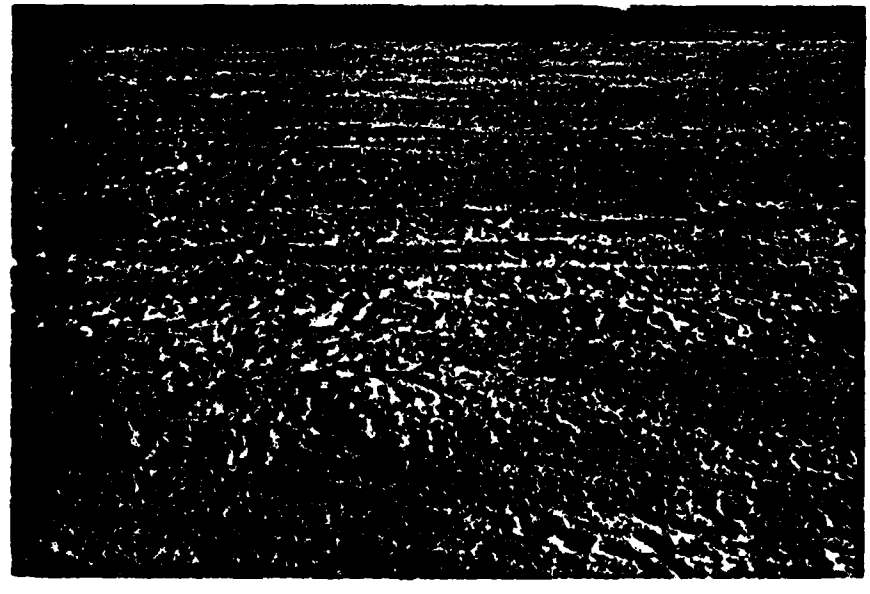

FIGURE 3.3:
Rough Snow on FYI

FIGURE 3.4
Snow Drifts and Hollows Caused by the Large-Scale Roughness of MYI

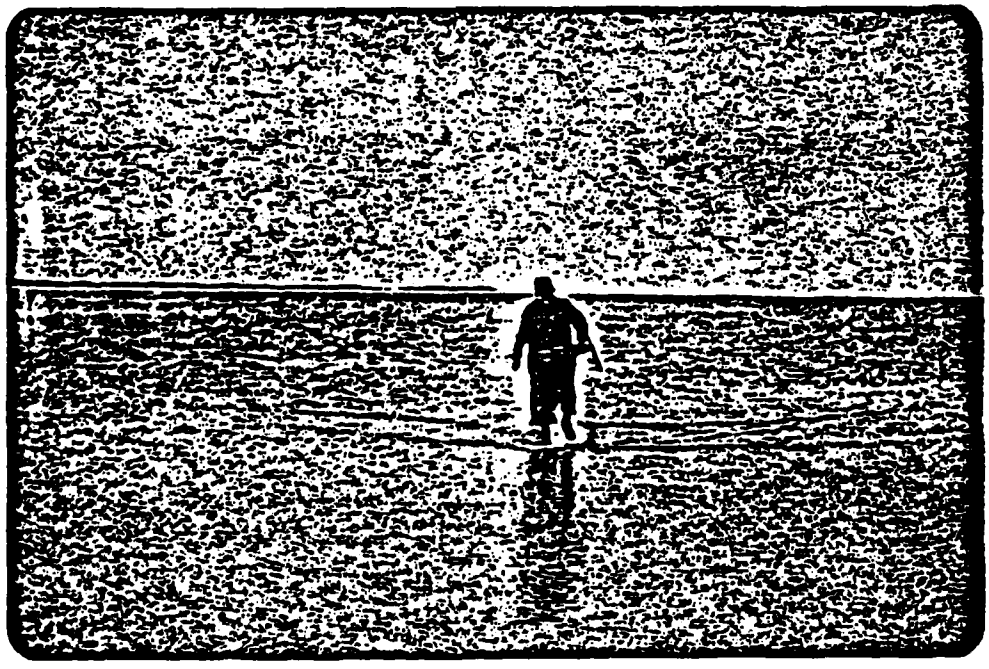

FIGURE 3.5
First-Year Ice Covered with Water in Rad Track Area South of Peach Pit Floe 29 June [Digby, 1982]

The size of the meltpools on June 28 increased compared to that on June 26 and the surface became wetter. The surface of FYI on July 2 was blue and the ice was saturated with water.

3.2.4 Pay Day

A multiyear floe with a refrozen lead was investigated in the Beaufort Byre pack ice near Hardinge Bay. MYI was weathered and had rounded peaks. The surface roughness on the hummocks ranged from smooth to slightly rough. Snow cover of varying depth was present on the ice, which was generally saturated.

By July 3, over 80% of the FYI was covered with water. The meltpool concentration also increased. A summary of the ice characterization data is given in Table 3.

TABLE 3
SUMMARY OF SITES INVESTIGATIONS AND COMMENTS ABOUT ICE CONDITIONS

			Depth		Temperature		Avg. Salinity		
Site	Type	Date	Ice (m)	Snow (m)	Air (°C)	Ice (°C)	top .10 °/oo	top .50 °/oo	Comments
Mould Bay	FY	06/21	2.25	0.02-0.01	2.2	0.1	1.54	2.84	Ice surface rough and has wet snow cover
		06/29	2.11	0.00	2.0	0.0	2.88	3.72	90% of surface area covered with water
Peach Pit	FY	06/22	1.88	0.02-0.05	2.5	0.0	1.16	3.06	Ice surface had varying degrees of roughness.
		07/02	1.83	0.0	4.0	0.0	2.30	3.11	Large portion of ice flooded
	MY	06/22	>3.0	0.01-0.02	2.5	0.0	0.05	0.19	Hummocks were wet and had small-scale roughnesses
Intre-pid	MY	06/26	>4.0	0.01-0.03	3.0	0.0	0.21	0.70	Hummocks were wet and smooth
Pay Day	MY	06/30	>4.0	0.01-0.02	4.2	0.0	0.17	0.18	Ice was saturated with water
	FY	07/03	1.00	0.00	4.0	0.0	2.10	2.80	Over 80% of surface covered with water.

4.0 PROFILES

A few selected profiles of the sites studied during this experiment are presented in this section. The scattering coefficient, σ^0, is presented as a function of the time taken to traverse the flight line.

The markers used to encode the different ice conditions and types from a site are shown in Figures 4.1 - 4.4. The box in the upper right-hand corner of each profile contains all the relevant information: frequency, polarization, site, and date. The vertical lines are used to indicate site markers. In some of the profiles the data were lost because the range tracker lost track. The signal received from the target has to be higher than the noise by more than 3 dB for satisfactory operation of the range tracker. When the received signal is close to internal noise the range tracker loses track. Missing data are indicated by a horizontal dashed line. Average

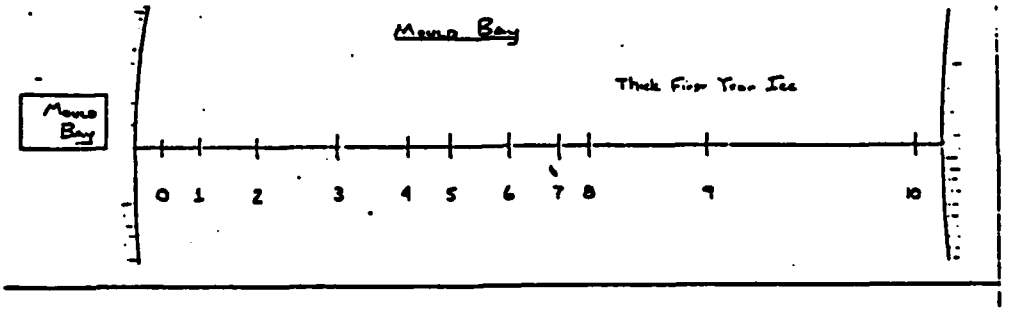

FIGURE 4.1: Relative Positions of Site Markers on Mould Bay Flight Line

scattering coefficients and standard deviations are also shown on these profiles.

Profiles acquired from Peach Pit on June 19 are shown in Figure 4.5. It is not possible to separate MYI from FYI at 12°, but the low backscatter at the beginning of the flight line indicates that this area is rough and this

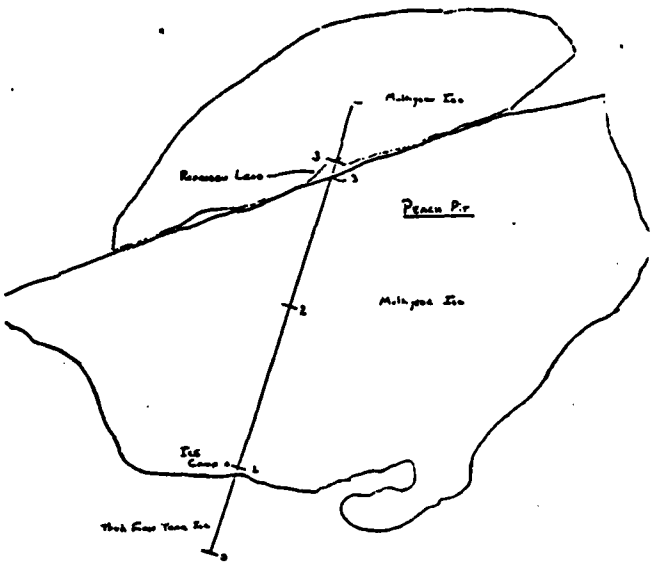

FIGURE 4.2: Relative Positions of Site Markers on Peach Pit Flight Line

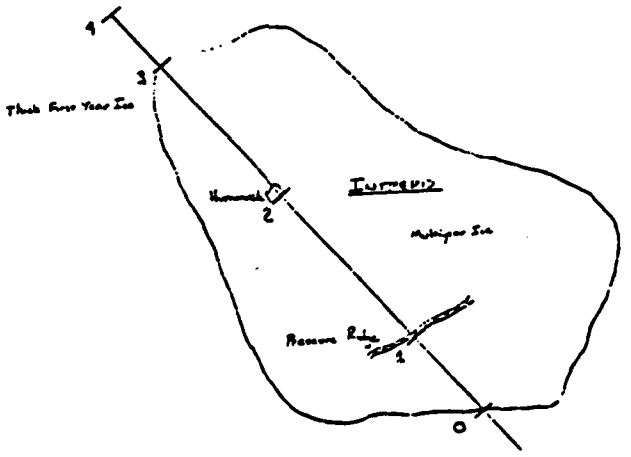

FIGURE 4.3: Relative Positions of Site Markers on Intrepid Flight Line

correlates with the surface observations. The variation in the backscatter from the lead is much lower than that surrounding MYI.

First-year ice can be easily distinguished from the multiyear ice at 30°. The backscatter from the ice covered with heavy snow cover (drift) is 2 dB lower than the average backscatter from FYI. Backscatter from the lead is 3 dB higher than surrounding MYI.

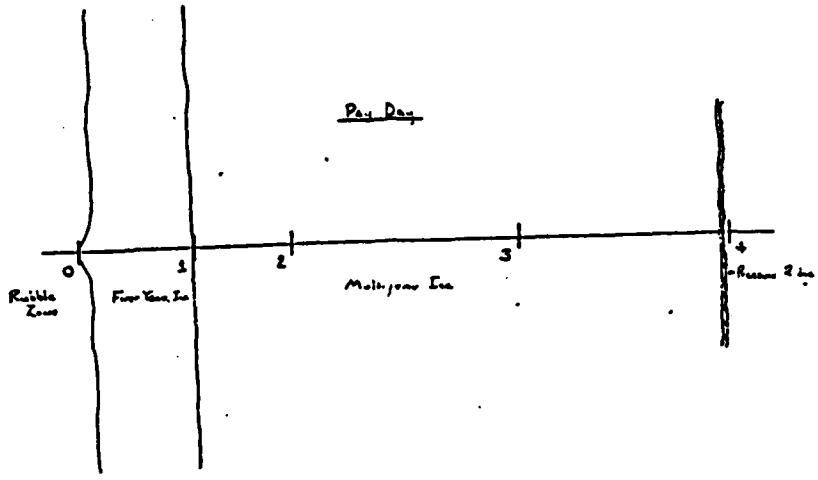

FIGURE 4.4: Relative Position of Site Markers on Pay Day Flight Line

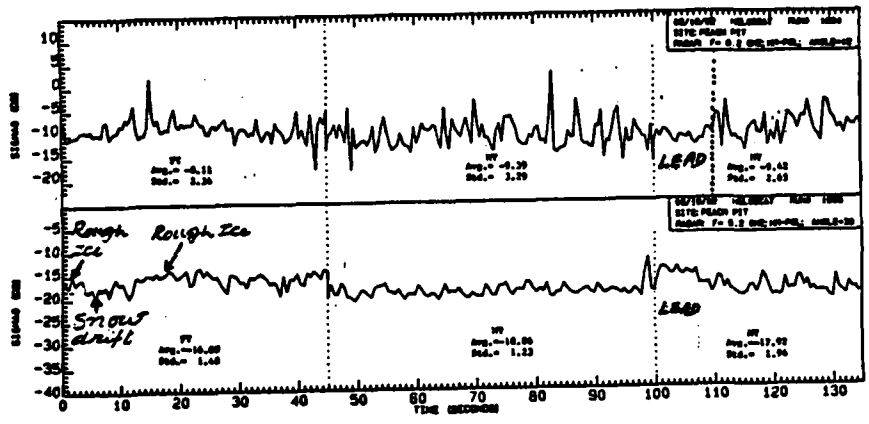

FIGURE 4.5: Profiles of First-Year and Multiyear Ice

The Mould Bay profiles shown in Figure 4.6 indicate that the surface is uniformly rough except at the beginning of the flight line.

The profiles of Peach Pit, acquired on June 22, are shown in Figure 4.7a. It is possible to distinguish FYI from MYI in these profiles. The high returns in MYI are caused by the edges of meltpools and hummocks; low returns are from the meltpools and areas with thick snow cover. Therefore, a

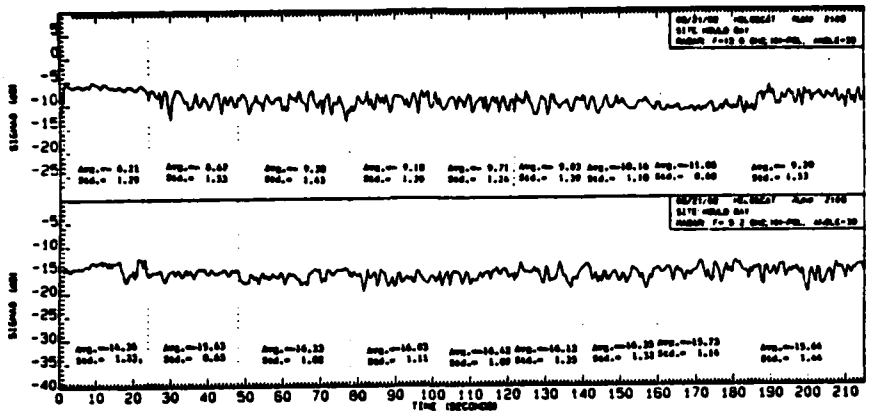

FIGURE 4.6: Profiles of First-Year Ice

profiling sensor can separate not only the basic ice types but also the different ice features in these basic types.

The profiles of Intrepid Inlet are shown in Figure 4.7b. Data collection became difficult and unreliable during this period because of the reduced backscatter from ice. It is not possible to distinguish the FYI from MYI with these profiles. It is also not possible to separate PR from the surrounding ice.

The profiles of Pay Day, collected on June 30, are shown in Figure 4.7c. It is not possible to distinguish the basic ice types from the profiles.

The Peach Pit profiles, acquired on July 2, are shown in Figure 4.8a. It is possible to distinguish basic types of ice from these profiles. Two distinct features of the FYI during this period are meltpools and drained areas. The backscatter from the drained areas is about 10-12 dB higher than that from pools. The high backscatter from the ice mounds indicates that the roughness elements may be comparable to wavelengths at higher frequencies in X-band.

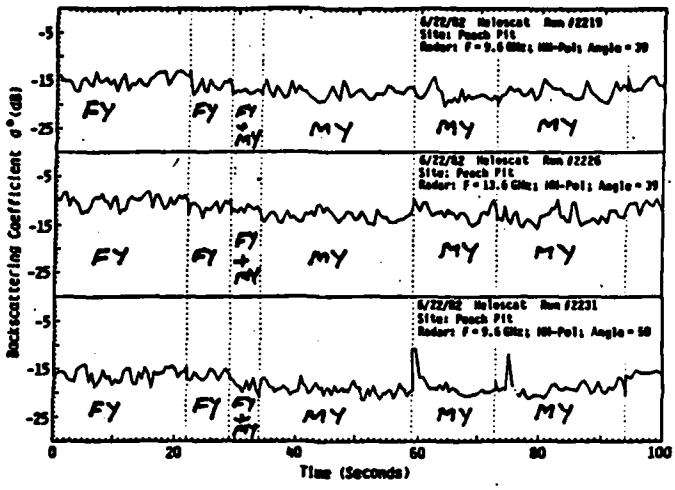

(a)

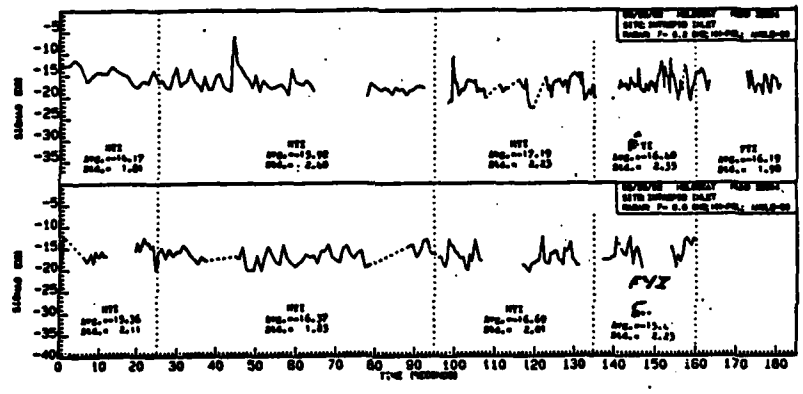

(b)

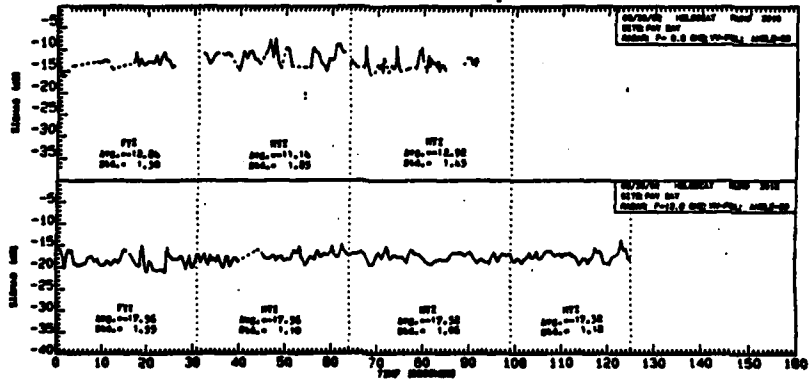

(c)

FIGURE 4.7: Profiles Under Summer Conditions. (a) Peach Pit, (b) Intrepid, (c) Pay Day

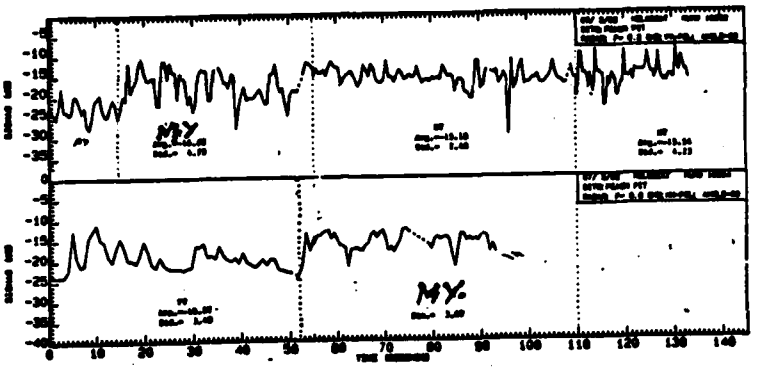

(a)

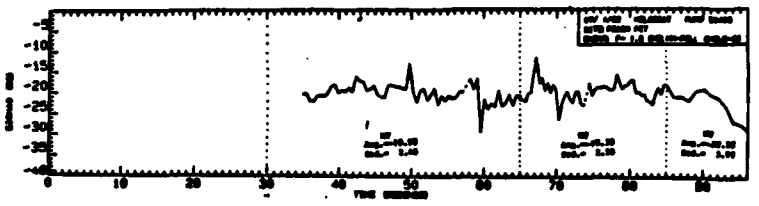

(b)

FIGURE 4.8: Profiles of First-Year and Multiyear Ice

Profiles of Peach Pit collected with the L-band system are shown in Figure 4.8b. The range tracker was able to track the signal from MYI, but was not able to track the signal from FYI. This indicates that the return from FYI is much lower than that from MYI. The ice mounds appear smooth to L-band radar and the backscatter from these areas is not much higher than that from pools. Therefore, L-band radar may be useful for distinguishing FYI from MYI during late summer.

Profiles of Intrepid at 1.5 GHz are shown in Figure 4.9. First-year ice can be distinguished from MYI in the profiles. The backscatter from MYI is

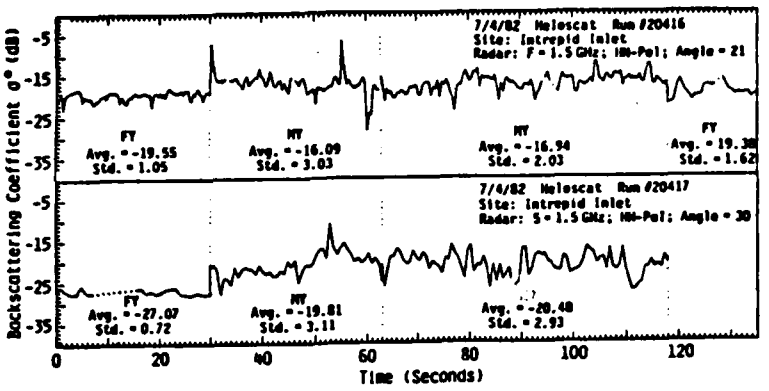

FIGURE 4.9: Profile of Intrepid Under Peak Summer Conditions

higher than from FYI. The contrast between FYI and MYI is 3.5 dB at 21° and 7.3 dB at 30°.

Distribution of the scattering coefficient for FYI and MYI during early summer is shown in Figure 4.9. The standard deviation for MYI is slightly larger than that for FYI. The distributions for FYI and MYI during summer overlap, as opposed to two distinct distributions during winter (see Figure 4.10). This is not unusual as the tails of the distribution for FYI and MYI overlap and this fills the nulls between the distributions.

The distribution of σ^0 for FYI and MYI during late summer is shown in Figure 4.11. The standard deviation for MYI (3.03 dB at 21° and approximately 3 dB at 30°) is much larger than that for FYI (1.05 dB at 21° and 0.72 dB at 30°) at 1.5 GHz (see Figure 4.12). The large standard deviation for MYI can be attributed to very low returns from the meltpools and wet snow, and high returns from the bare ice (hummocks). Large areas of FYI are covered with meltpools and a few ice mounds. The backscatter from the ice mounds is not much larger than that from water at L-band. Therefore, it may be possible to separate MYI from FYI based on the distributions.

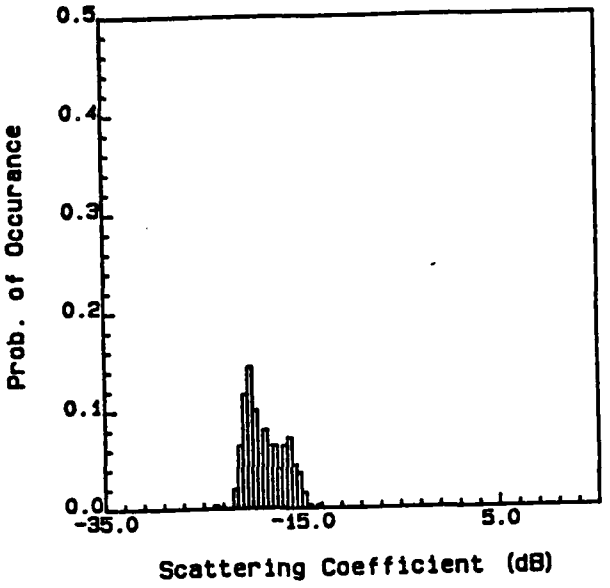

FIGURE 4.10: Distribution of σ^0 for FYI and MYI at Peach Pit During Summer

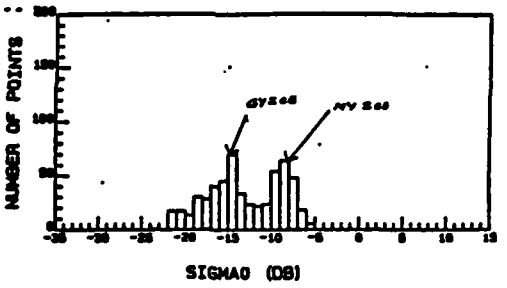

FIGURE 4.11: Distribution of σ^0 for Grey and Multiyear Ice During Summer

5.0 FREQUENCY AND ANGULAR RESPONSES

The backscatter data were analyzed to obtain the angular and frequency responses for the basic types of ice. As mentioned earlier, full-length profiles of the site were acquired at a few selected frequencies; backscatter measurements at other frequencies are made by stepping the center frequency atregular intervals with the helicopter flying along the selected flight line. Scatter in the mean scattering cross-sections is due to the small number of independent samples and the spatial inhomogeneity of the ice. A weighted regression analysis based on the number of independent samples

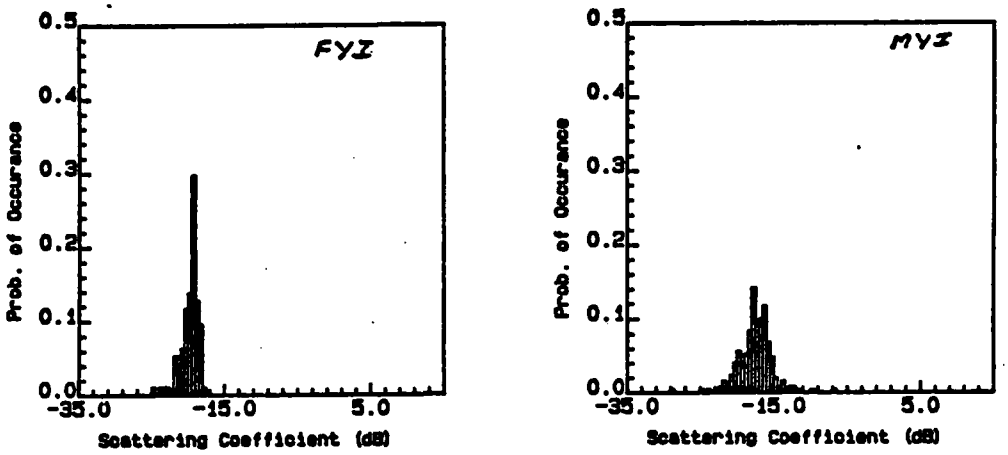

(a)

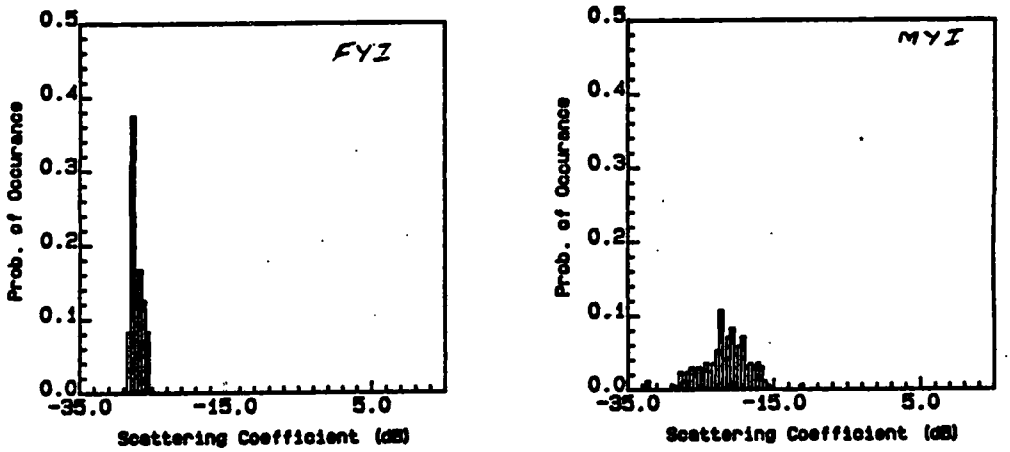

(b)

FIGURE 4.12: Distribution of σ^0 of FYI and MYI at Intrepid During Late Summer. (a) 1.5 GHz, 20°; (b) 1.5 GHz, 30°

available at each frequency was performed to remove scatter due to fading and target inhomogeneities.

The data set is divided into three groups for further discussion in this section: (1) early summer (June 19-June 24), (2) mid-summer (June 26-June 30), and (3) late summer (July 2-July 3).

5.1 Angular Response

The angular response of the backscatter from FYI and MYI at selected frequencies fro.. different sites during the early summer is shown in Figures 5.1a - g. The angular response of FYI is similar to that from a moderately

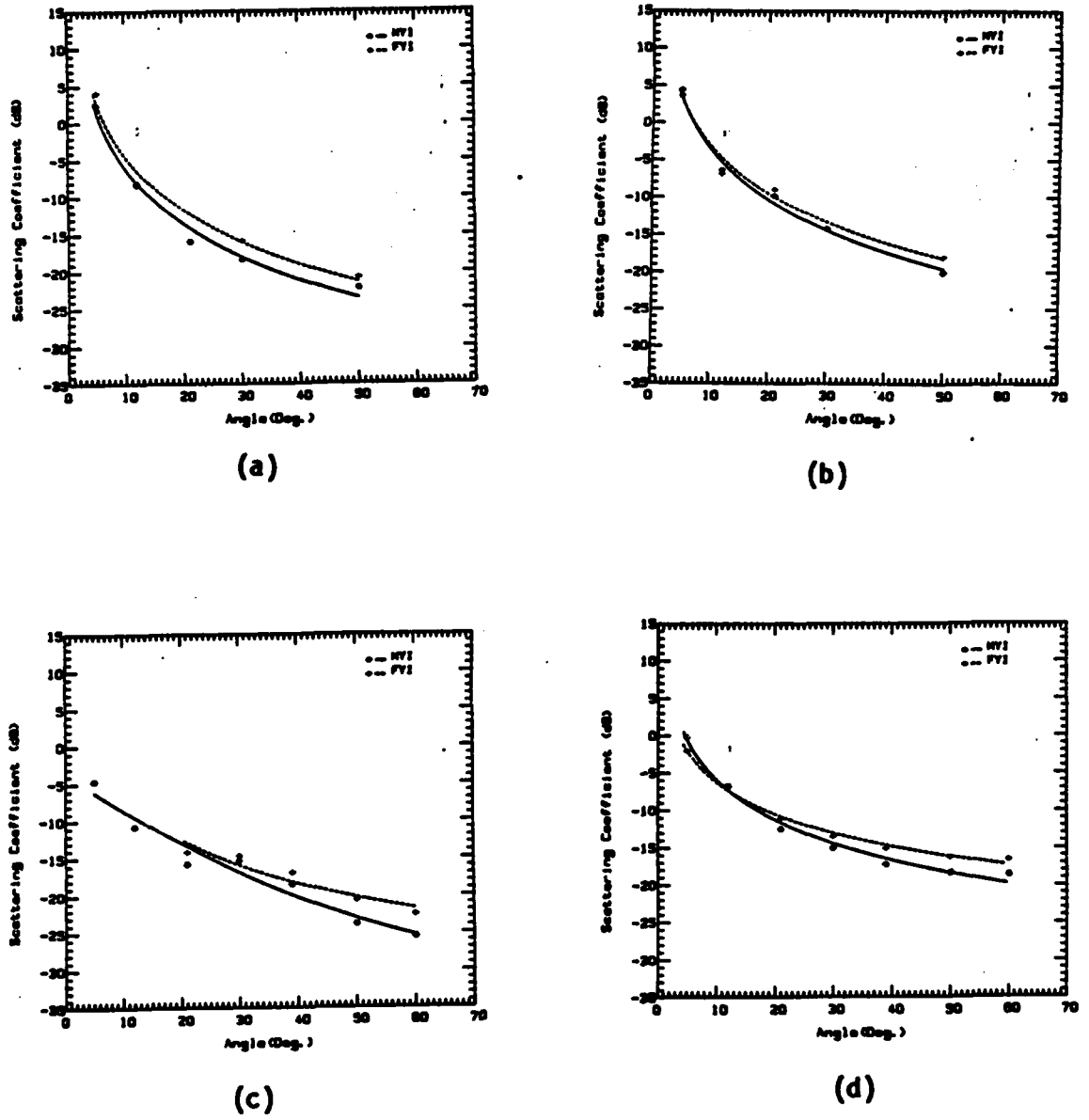

FIGURE 5.1: Scattering Coefficient of First-Year and Multiyear Ice.
(a) 5.2 GHz, HH-Pol., June 19; (b) 9.6 GHz, HH-Pol., June 19;
(c) 5.6 GHz, HH-Pol., June 22; (d) 9.6 GHz, HH-Pol., June 22.

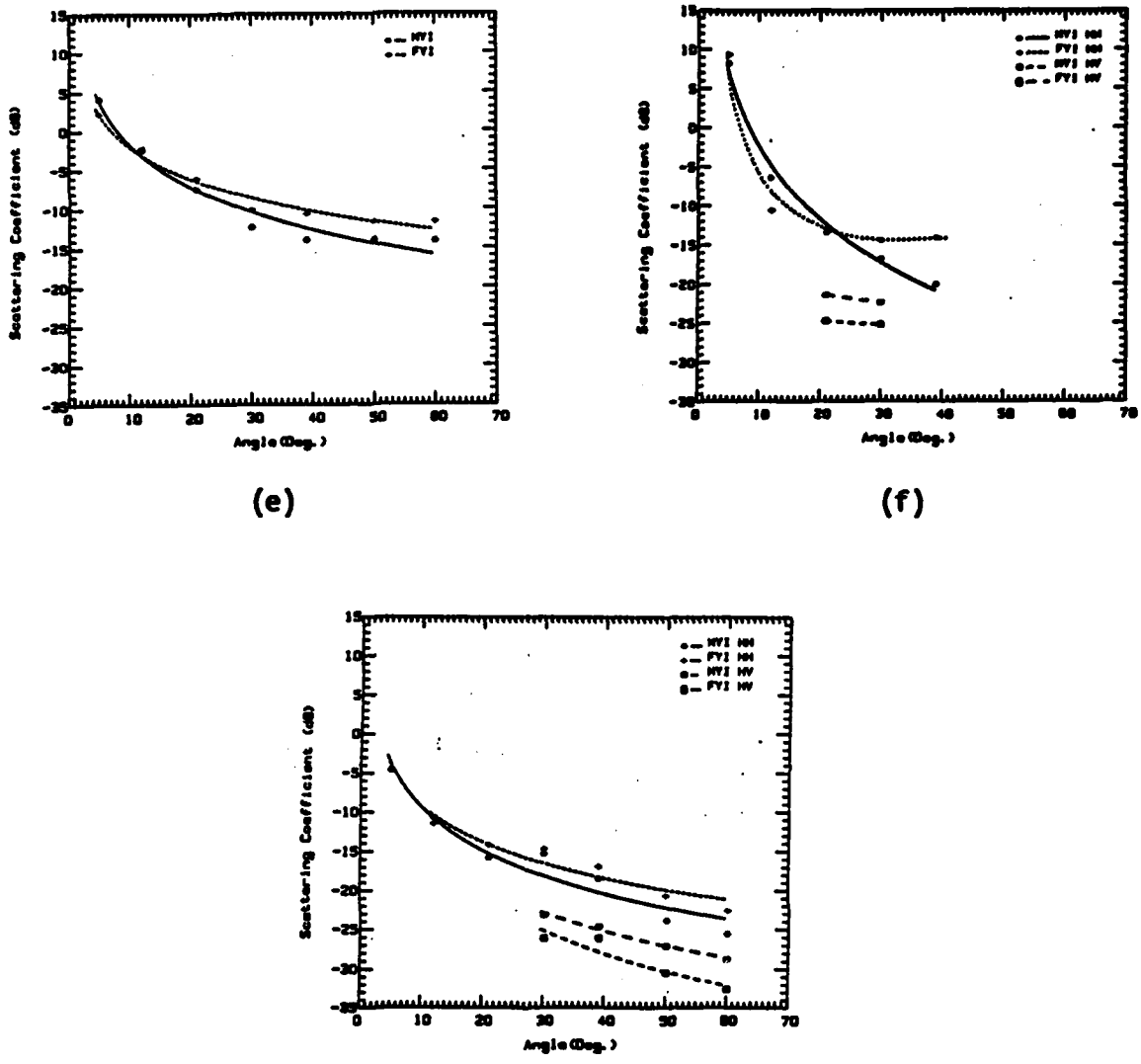

FIGURE 5.1: Scattering Coefficient of First-Year and Multiyear Ice. (e) 13.6 GHz, HH-Pol., June 22; (f) 5.2 GHz, HH, HV-Pol., June 24, Peach Pit (g) 5.6 GHz, HH, HV-Pol., June 22.

rough surface (Figure 5.1b). Illustrations of the changes in FYI during summer are shown in Figure 5.2. During pre-melt conditions, the ice surface is covered with humid snow and the surface roughness of ice is generally small

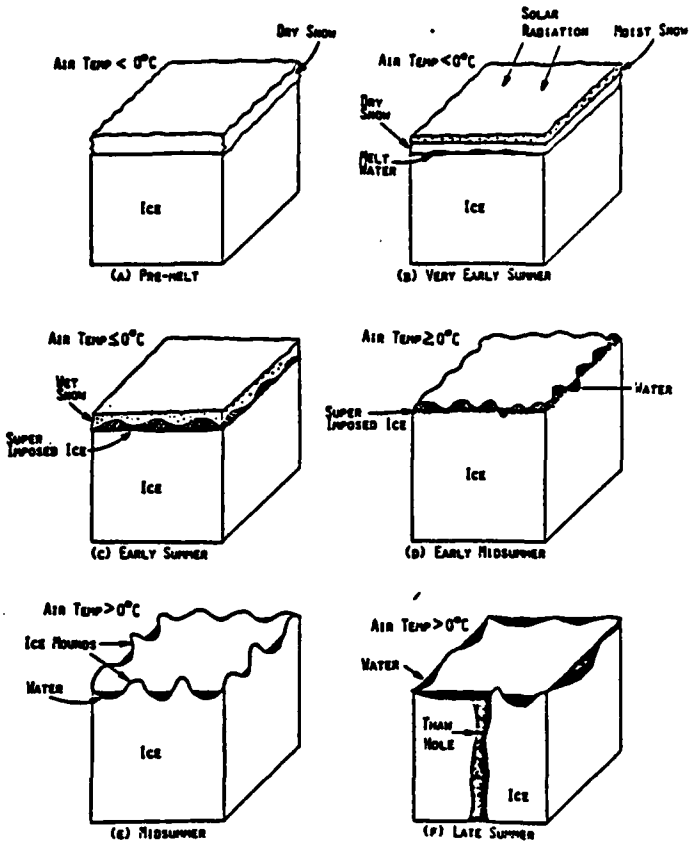

FIGURE 5.2: First-Year Ice

(less than 0.2 cm). During early summer, the incoming solar radiation is absorbed by the upper layers of snow, causing these layers to be warmed to temperatures near the melting point. These upper layers of snow are wet and melting occurs with further heating. The melt water percolates to the surface of the ice and refreezes there. This is called superimposed ice [Jacobs, 1975]. The surface roughness increases dramatically because of this superimposed ice, as shown in Figures 5.3 - 5.4. The increased backscatter from the ice surface is reduced by wet snow. Melting and refreezing of the snow also causes an increase in surface roughness. The backscatter from FYI during early summer increases because of these effects. An illustration of MYI

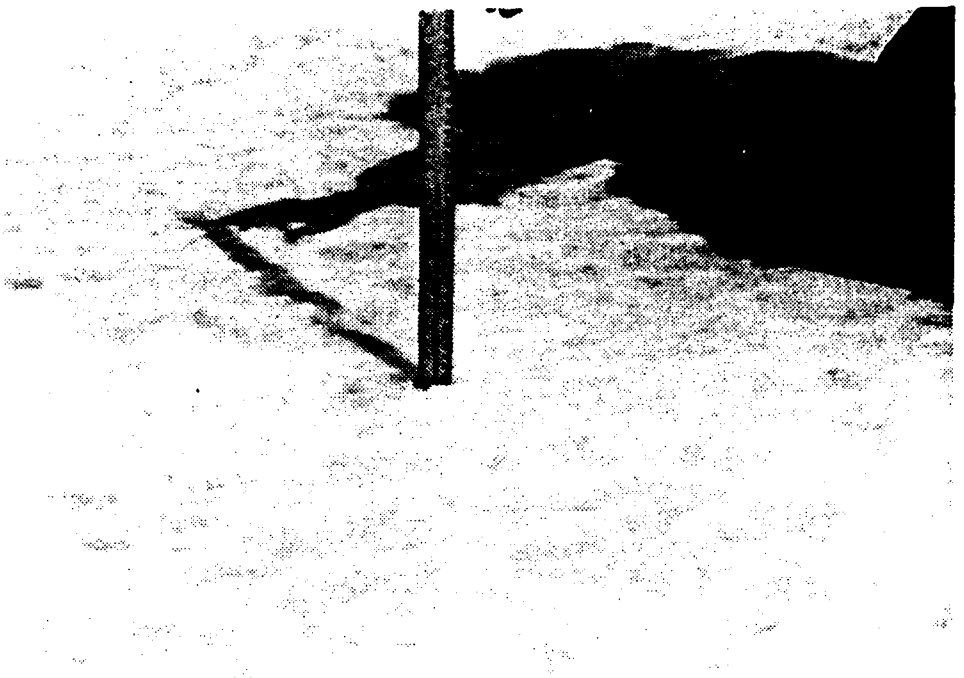

FIGURE 5.3: Typical Surface Roughness of FYI on Peach Pit

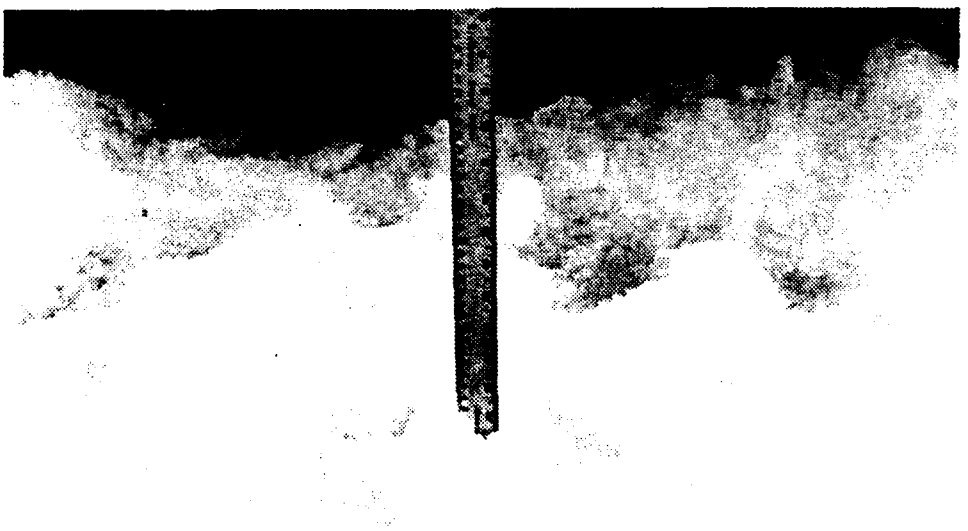

FIGURE 5.4: Surface Roughness of FYI During Early Summer

during winter and summer is shown in Figure 5.5. During early summer, the surface of MYI is made up of hummocks, wet snow and meltpools, and is saturated with water. The volume scatter contribution from MYI is reduced because of the presence of water in the ice and wet snow on the surface. Generally superimposed ice on MYI forms below the heavy snow pack; the superimposed ice does not influence the backscatter return because of the masking effect of the thick wet snow. Depth of snow cover on the hummocks is generally much smaller than that required for superimposed ice formation. The large-scale roughness of MYI causes melt water to be collected in the depressions from melting snow and consequent formation of meltpools on MYI much faster than on FYI. Therefore, the backscatter from MYI is less than that during winter.

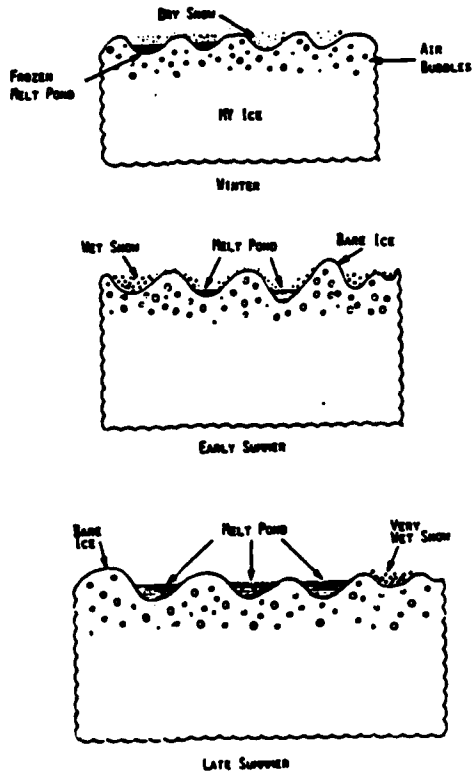

FIGURE 5.5: Multiyear Ice

There is a small difference in the average scattering cross-section of MYI and FYI at angles larger than 20° at 5.6, 9.6 and 13.6 GHz (Figures 5.1a-f). Therefore, a scatterometer may be useful for distinguishing the basic types of ice during the early summer. The incidence angle should be larger than 30° and a large number of independent samples must be averaged to obtain a precise estimate of the scattering coefficient.

The angular response of scattering coefficient at selected frequencies from different sites during mid-summer is shown in Figures 5.6 - 5.7. The

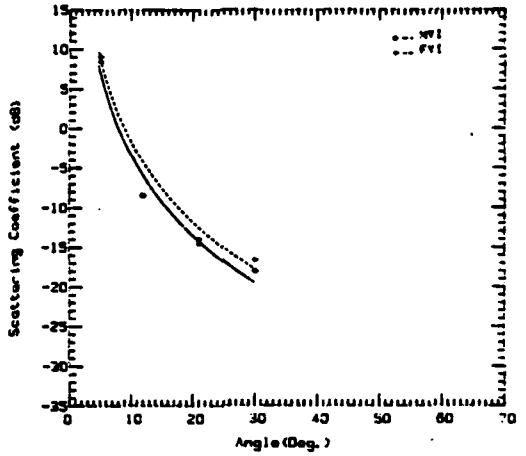

(a)

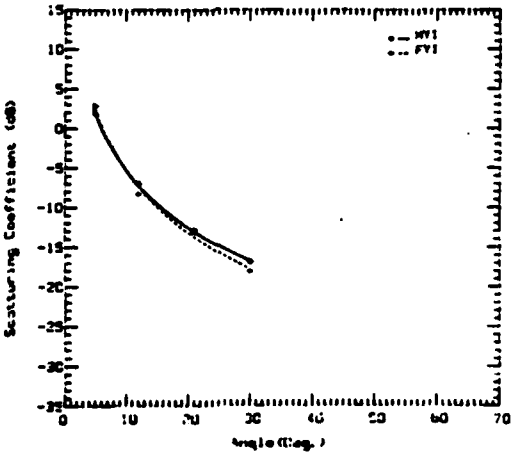

(b)

FIGURE 5.6: Scattering Coefficient of First-Year and Multiyear Ice, June 26, Intrepid; (a) 5.2 GHz, HH-Pol.; (b) 9.6 GHz, HH-Pol.

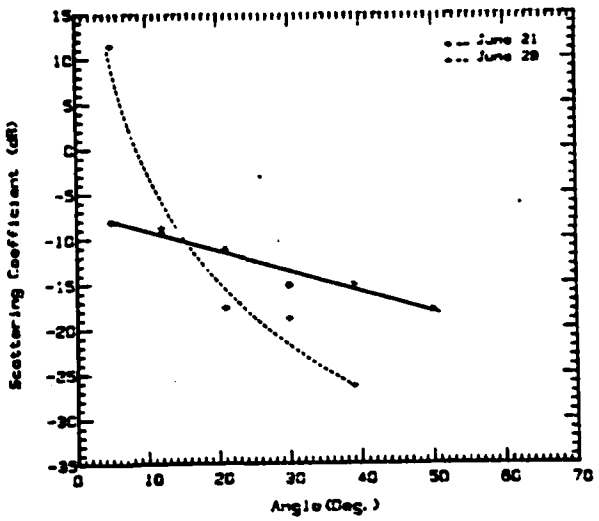

FIGURE 5.7: Scattering Coefficient of First-Year Ice at 5.2 GHz, HH-Pol., Mould Bay

scattering coefficient decrease with incidence angle is similar to that from a smooth surface. The surface of the ice on the hummocks was smooth, and snow cover in the depressions and valleys of the ridge was wet and granular. The percentage of meltpools on MYI also increased during this period. The backscatter from FYI was reduced because the surface was covered with wet snow and water. There is a 6.5 - 11 dB reduction in the backscatter from FYI at angles greater than 20° at Mould Bay (Figure 5.7). There is also a 20 dB increase in the backscatter at 5°. Over 80-90% of the FYI surface was covered with water during the backscatter measurements from this site.

The FYI and MYI scattering cross-sections for late summer at selected frequencies are shown in Figures 5.8a - c. The backscatter from FYI is further reduced because of the presence of water. The surface of the ice can, due to the rapid decay in the angular response, be seen as smooth by the radar during this period. There is a small contrast between MYI and FYI which increased with decreasing frequencies.

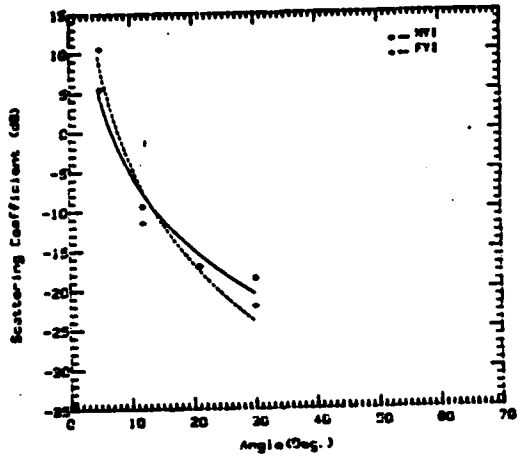

(a)

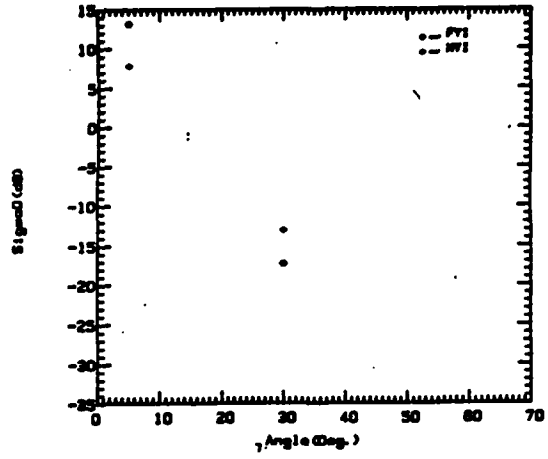

(b)

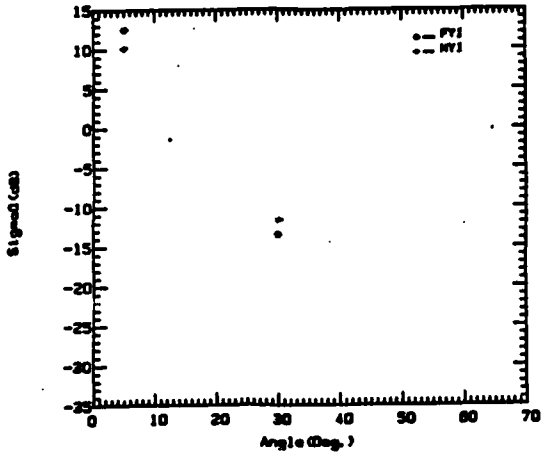

(c)

FIGURE 5.8: Scattering Coefficient of First-Year and Multiyear Ice
(a) 5.2 GHz, HH-Pol., July 2, Peach Pit;
(b) 9.6 GHz, HH-Pol., July 2, Intrepid;
(c) 13.6 GHz, HH-Pol., July 2, Intrepid.

5.2 L-Band Results

The angular response of backscatter at 1.5 GHz with HH-polarization for Intrepid is shown in Figure 5.9. The contrast between FYI and MYI is 3.5 and 7.0 dB at 21° and 30°, respectively. L-band radar is insensitive to small-

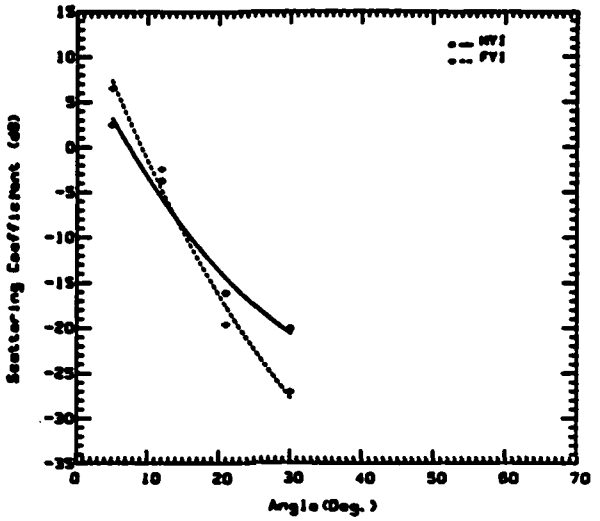

FIGURE 5.9: Scattering Coefficient of First-Year and Multiyear Ice at 1.5 GHz, HH-Pol., July 3, Intrepid

scale roughness of the drained areas and the backscatter from these drained areas is much lower than the higher frequencies in the C-, X- and Ku-bands. Therefore, it can be concluded that L-band is useful for distinguishing the basic types of ice during late summer.

5.3 Frequency Response

Spectral response of the scattering coefficient at selected angles from different sites during early summer is shown in Figures 5.10a - e. The scattering coefficient is generally found to increase with frequency. There is a small contrast between FYI and MYI during this period. The backscatter from FYI is slightly higher than from MYI. Operation with cross-polarization improved the contrast by 1-2 dB (Figure 5.10e).

The spectral response of σ^0 during mid-summer is shown in Figures 5.11a - c. The contrast between FYI and MYI during this period when the surface of the ice was very wet, is negligible for all polarizations. Multiyear ice consists of three features during this period: (1) meltpools; (2) bare ice

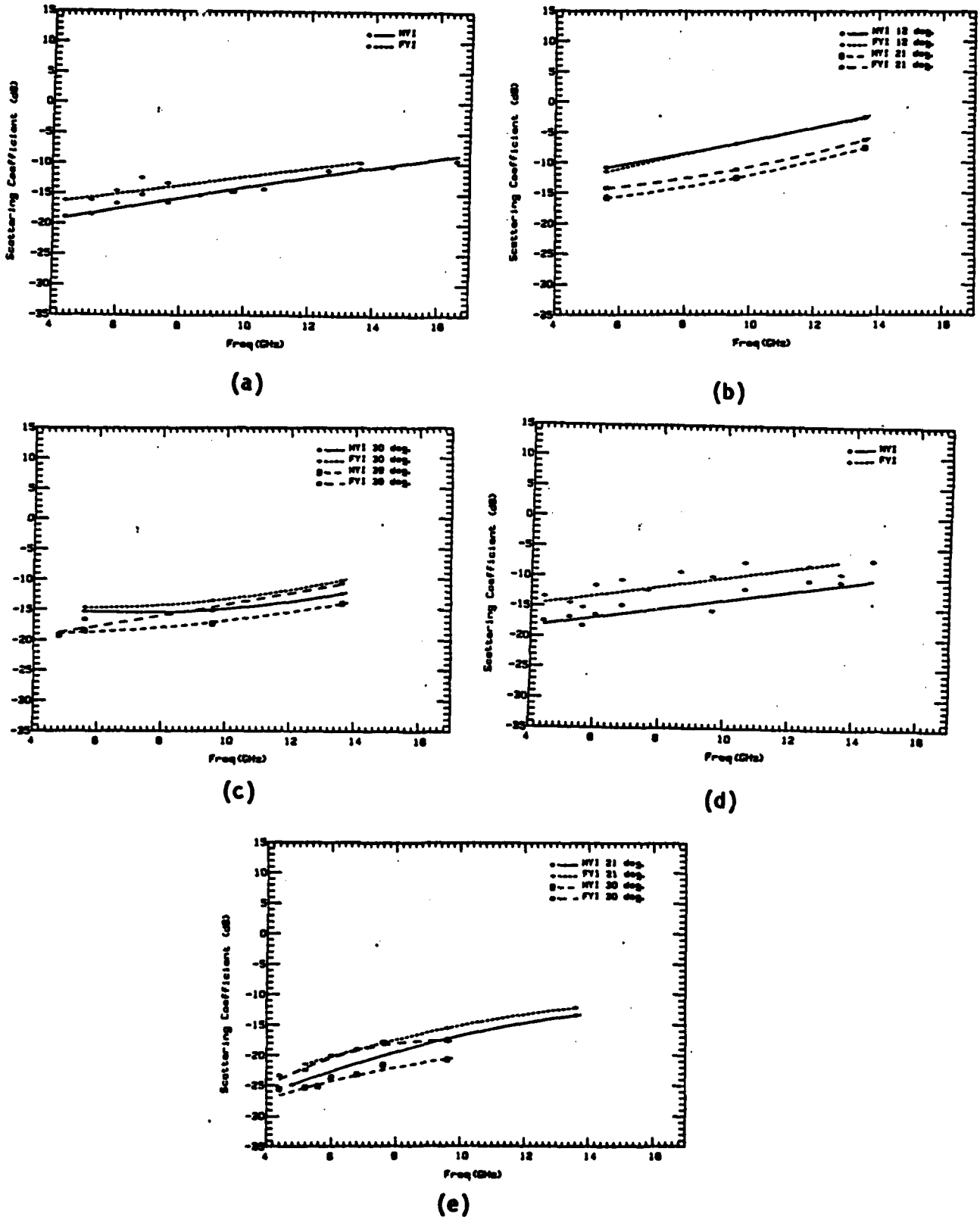

FIGURE 5.10: Scattering Coefficient of First-Year and Multiyear Ice. (a) 30°, HH-Pol., June 19; (b) 21°, HH-Pol., June 22; (c) HH-Pol., June 22; (d) 30°, HH-Pol., June 24; (e) HV-Pol., June 24.

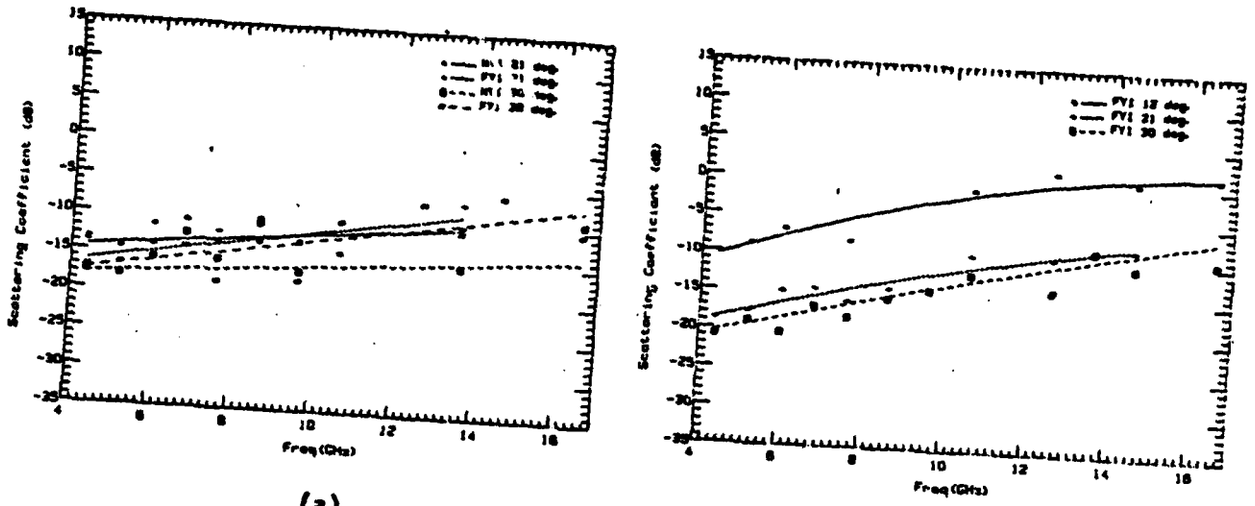

(a)

(b)

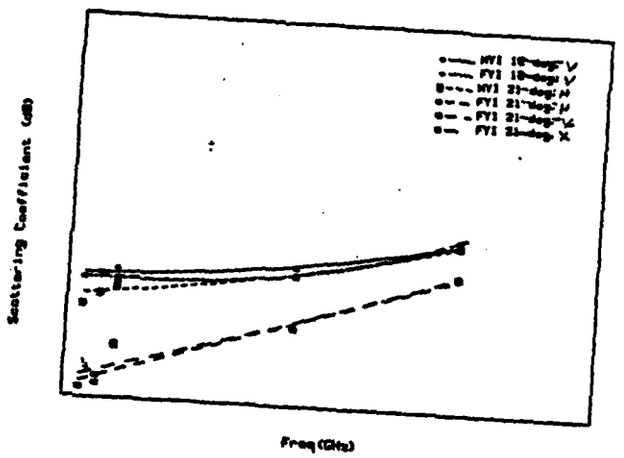

(c)

FIGURE 5.11: Scattering Coefficient during Mid-Summer. (a) First-Year and Multiyear Ice, HH-Pol., June 26, Intrepid; (b) First-Year Ice, HH-Pol., June 29, Mould Bay; (c) First-Year and Multiyear Ice, 30°, HH-Pol., July 30, Pay Day

(hummocks) and (3) wet snow (drifts). Two distinct features of first-year ice are: (1) meltpools and (2) ice mounds. The surface area covered by meltpools and snow wetness in the drifts increases as summer progresses. Surface area covered by pools is larger on FYI because of its smoother surface. Therefore,

the backscatter from FYI decreases more rapidly than that from MYI. The spectral response of the σ^0 during late summer is shown in Figures 5.12a - c. The backscatter from the FYI during this period is lower than that from MYI. During this period 80% - 90% of FYI surface is covered with water. This causes the backscatter from FYI to decrease. There is also a small contrast between FYI and MYI during this period. The contrast is larger at lower frequencies in the L- and C-bands.

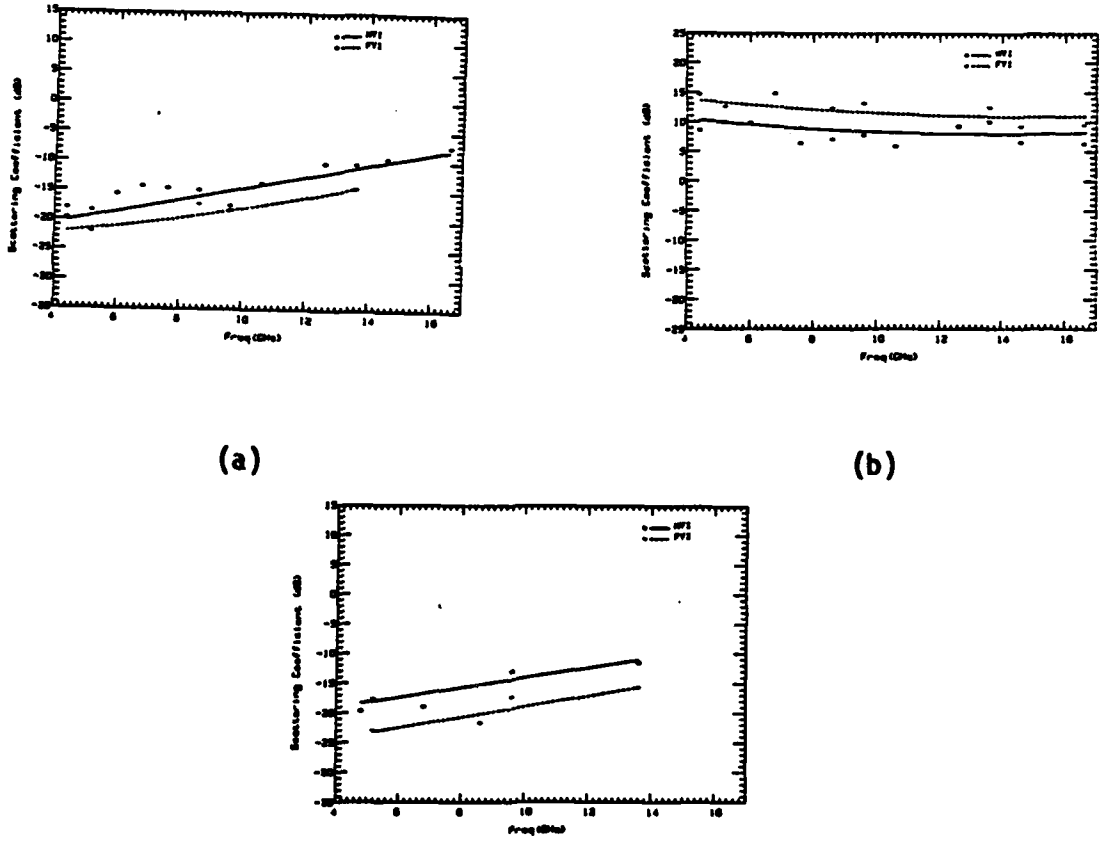

(a)

(b)

(c)

FIGURE 5.12: Scattering Coefficient of First-Year and Multiyear Ice. (a) 30°, HH-Pol., July 2, Peach Pit; (b) 5°, HH-Pol., July 2, Intrepid; (c) 30°, HH-Pol., July 2.

6.0 COMPARISON OF BACKSCATTER FROM DIFFERENT SITES

Comparison of the backscatter from different sites is presented in this section. The backscatter measurements from different sites were not made on the same day because of logistics problems.

The scattering coefficient of FYI from Mould Bay and Peach Pit is shown in Figure 6.1a. The backscatter from the FYI at Mould Bay is 2-3 higher than that from Peach Pit. The backscatter measurements from Mould Bay and Peach

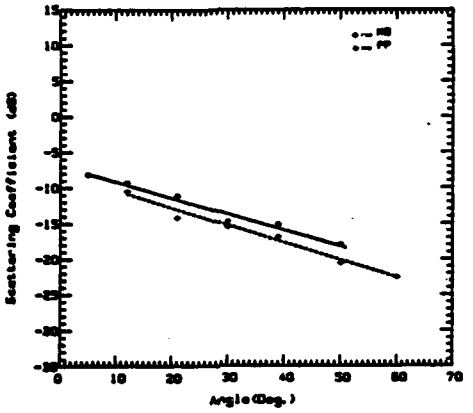

(a)

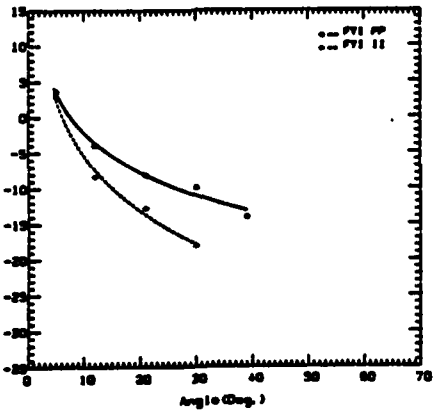

(b)

FIGURE 6.1: **Scattering Coefficient of First-Year Ice. (a) 5.2 GHz, HH-Pol., June 21-22; (b) 9.6 GHz, HH-Pol., June 24 and 26.**

Pit were made on June 21 and June 22, respectively. The surface of the FYI at Mould Bay is slightly rougher than that at Peach Pit. The higher backscatter from Mould Bay could be because of the difference in the surface roughness or different melting rates on these sites.

The backscatter from FYI at Peach Pit and Intrepid is shown in Figure 6.1b. The backscatter measurements were made on June 24 and June 26 at Peach Pit and Intrepid, respectively. The backscatter from FYI at Intrepid is about 8 dB lower than that at Peach Pit. There was a large increase in the melt water on the surface of the FYI on June 26. The reduction of snow cover on the FYI on June 24 exposed the superimposed ice. This caused a slight increase in the backscatter from the FYI at Peach Pit.

The backscatter from MYI at Peach Pit and Intrepid at 9.6 GHz is shown in Figure 6.2a. The backscatter from MYI at Peach Pit was 2-3 dB higher than that at Intrepid. The MYI at Intrepid was more weathered and had rounded peaks. In addition, the surface of the ice was wetter, which might have caused further reduction of the volume scatter from MYI.

The backscatter from MYI at Peach Pit and Intrepid on July 2, 1982 is shown in Figure 6.2b. The backscatter from ice at Peach Pit is slightly higher than from the ice at Intrepid. This could be because of the different wetness distributions on the site.

The backscatter from MYI at Peach Pit at 5.2 and 9.6 GHz is shown in Figures 6.2c and d. There is a negligible difference in the backscatter from early summer to late summer at 9.6 GHz. There is more than 10 dB difference at 5.2 GHz at 5° between June 22 and 24. The backscatter on June 24 is higher than that on June 22 at incidence angles lower than 30° and lower than June 22 at incidence angles greater than 25°. This indicates an increase in the size of meltpools on June 24.

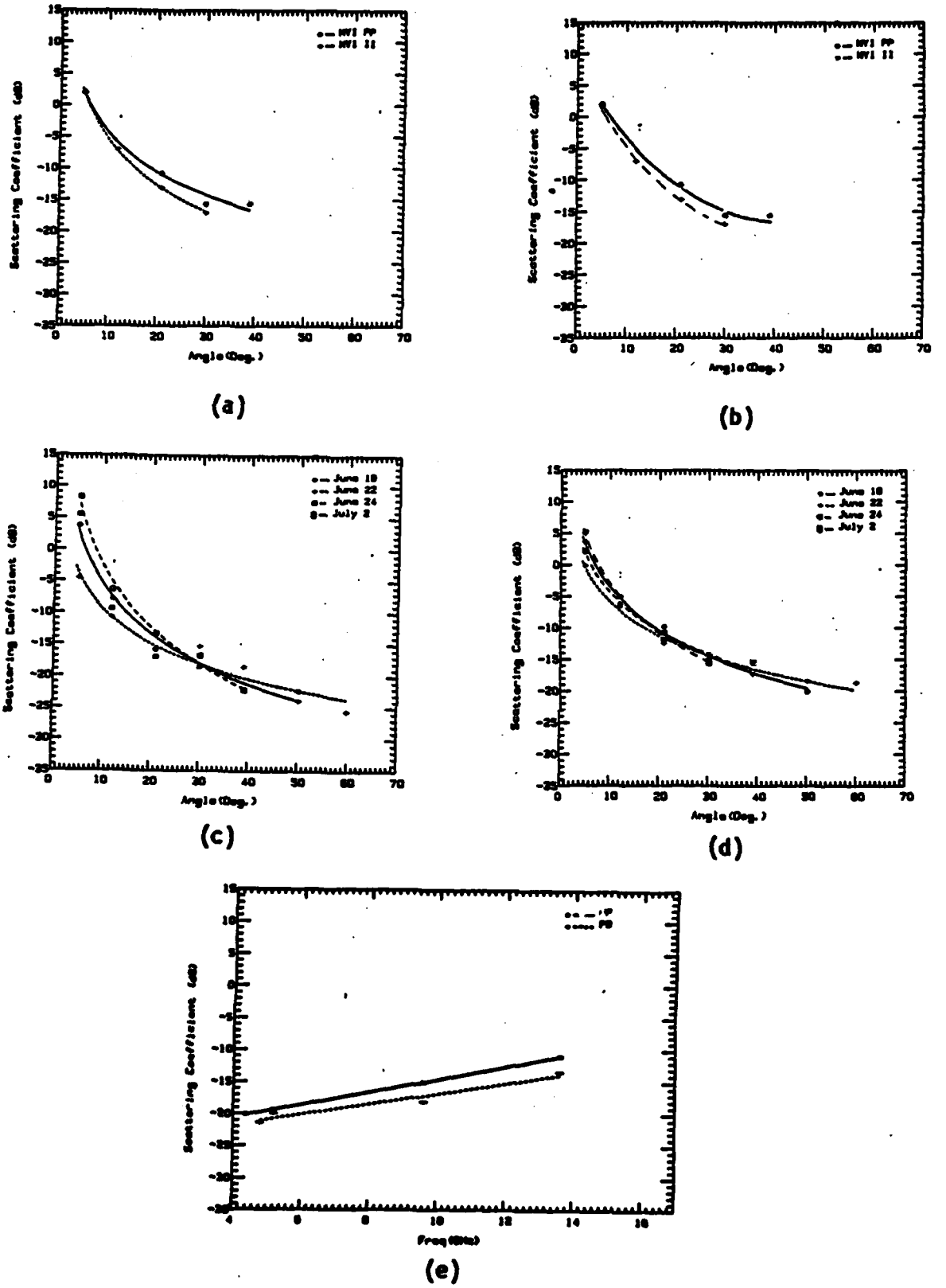

FIGURE 6.2: Scattering Coefficient of Multiyear Ice, HH-Pol. (a) 9.6 GHz, June 24 and 26; (b) 5.2 GHz, July 2; (c) 5.2 GHz, Peach Pit; (d) 9.6 GHz, Peach Pit; (e) 30°.

The backscatter from MYI on Intrepid and Pay Day is shown in Figure 6.2e. There is a negligible difference between the backscatter from the two sites at 5.2 GHz. The backscatter from MYI on Peach Pit is about 2-3 dB higher than that from MYI on Pay Day at 9.6 and 13.6 GHz.

7.0 COMPARISON OF SUMMER AND FALL DATA

The physical and electrical properties of sea ice change during summer. During summer the ice surface initially is covered with wet snow and ice. As summer progresses, meltpools are formed on the surface of the sea ice because of the melting snow and, eventually, the surface of the ice. The depth of penetration of electromagnetic waves decreases by an order of magnitude because of the presence of the small amount of liquid water in the snow over that for dry snow. The salinity of the ice changes during summer because the melt water percolates through the surface layers at the same time entraining some brine. The radar backscatter from sea ice is different from other seasons because of these reasons. In this section a few selected profiles and angular responses of summer and fall are compared.

The profiles acquired during fall (1981) and summer (1982) are shown in Figures 7.1a and b. The backscatter from FYI in summer is similar or slightly higher than that during fall. The backscatter from MYI during summer is less than that during fall, as shown in Figures 7.1a and b. The reduction in backscatter from MYI is because of reduced volume scatter caused by the presence of wet or humid snow and ice on the surface. The backscatter from the FYI is higher than that from MYI during summer as opposed to a lower value during fall. As summer progresses, the backscatter from FYI reduces, eventually becoming lower than MYI. This is caused by presence of meltpools and a

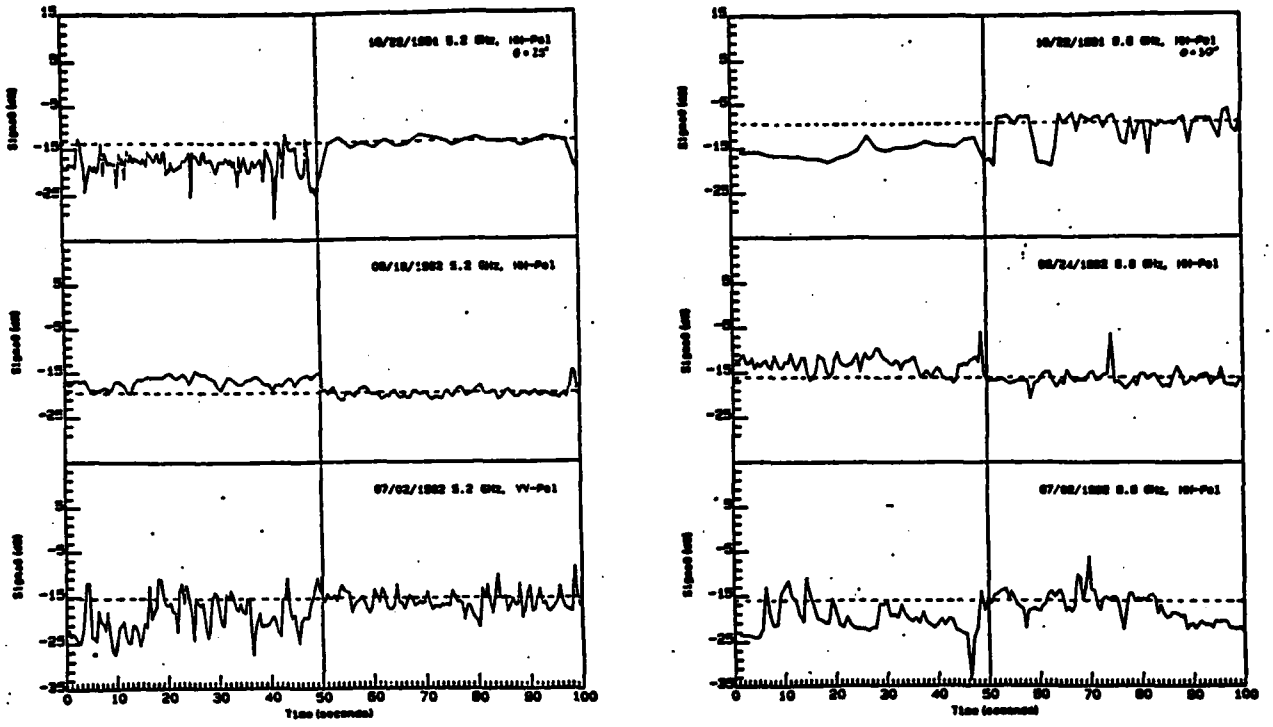

(a) (b)

FIGURE 7.1: First-Year and Multiyear Ice During October, Early Summer and Two Weeks Later. (a) 5.2 GHz, 30°; (b) 9.6 GHz, 30°.

reduction in surface roughness because of the presence of water on the ice during late summer.

The average σ^0 of FYI during fall (1981) and summer (1982) at 5.2 GHz and 9.6 GHz is shown in Figures 7.2a and b, respectively. The average scattering coefficient from FYI during summer is about 5 dB higher than than during fall at 5.2 GHz and incidence angles larger than 10°. The average scattering coefficient of FYI at 9.6 GHz at incidence angles greater than 10° during summer is slightly higher (about 2.5 dB) than that during fall.

The average σ^0 of MYI during fall ('81) and summer ('82) at 5.2 and 9.6 GHz is shown in Figures 7.3a and b, respectively. Backscatter from MYI during summer at 5.2 and 9.6 GHz, and incidence angles larger than 20° is lower than

that during fall. The difference is higher at 9.6 GHz, which again indicates that there is a significant reduction in the volume scatter from MYI during summer.

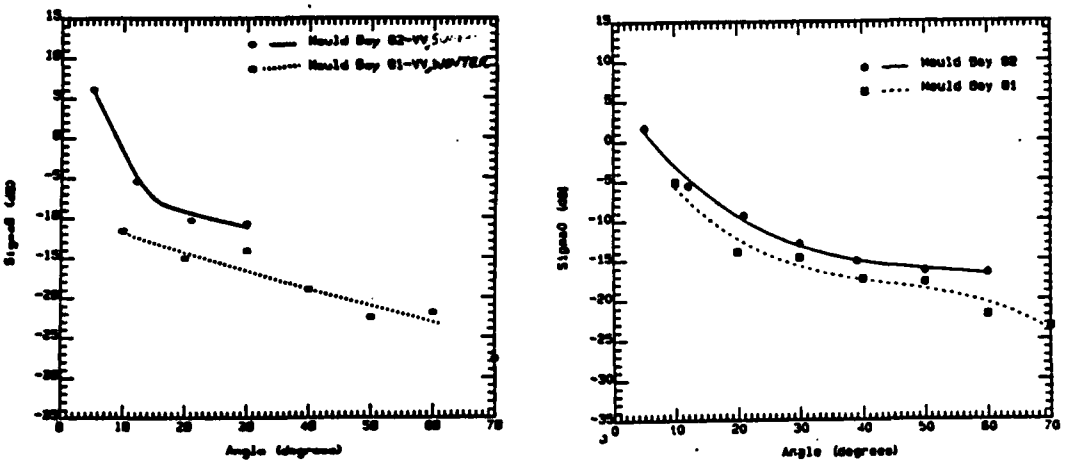

(a) (b)

FIGURE 7.2: Angle Response of First-Year Ice. (a) 5.2 GHz; (b) 9.6 GHz

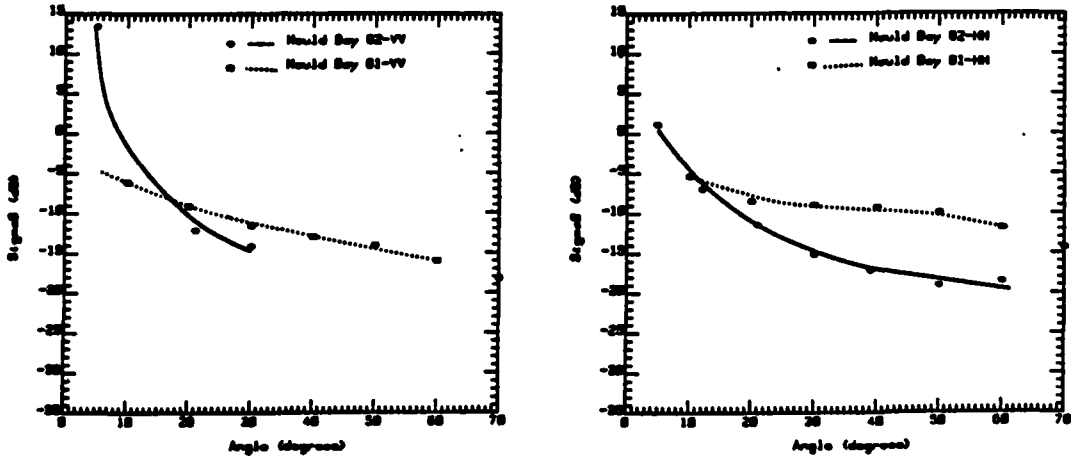

(a) (b)

FIGURE 7.3: Angle Response of Multiyear Ice. (a) 5.2 GHz; (b) 9.6 GHz.

8.0 CONCLUSIONS AND RECOMMENDATIONS

The significant achievement of this experiment was to advance the knowledge of radar backscatter from sea ice during summer. The information gained is useful in designing radar systems for monitoring sea ice, planning future experiments, and understanding the scattering mechanism. In this section general conclusions, problems and recommendations are presented.

8.1 Conclusions

The general conclusions from this experiment are:

(1) A scatterometer may be useful for discriminating FYI from MYI during the early part of summer when the ice surface is covered with wet snow. The contrast is generally small at all frequencies; therefore, the σ^0 has to be measured with high precision (100 or more independent samples must be averaged to reduce fading).

(2) The radar backscatter from FYI is slightly higher than that from MYI during the early part of the summer but becomes lower than that from MYI as summer progresses.

(3) The radar backscatter from FYI is slightly higher than that during fall. The σ^0 of MYI during summer is lower than during fall because of reduced volume scatter from it.

(4) It is possible to monitor the onset of melting by observing the same piece of MYI continuously throughout the year.

(5) It may be possible to monitor the melting of snow or ice by continuously observing the same piece of FYI during summer.

(6) It is not possible, based on the average scattering coefficient, to distinguish MYI from FYI over a short period

during summer, although it may be possible to distinguish FYI from MYI from the meltpool concentrations.

8.2 Problems

(1) One of the major problems during this experiment was to reduce the radar's sensitivity because of the interference from the helicopter. The minimum measurable σ^0 when the radar was operated on the ground and from the helicopter is shown in Tables 4 and 5, respectively. As can be seen from these tables, there was a 5 - 20 dB loss in sensitivity when using the helicopter. This made measurements at large incidence angles difficult and unreliable. It was not possible to solve this problem during the experiment because of lack of adequate test equipment and time.

(2) Backscatter measurements for some frequencies and polarizations were not made because of lack of time. The measurements with cross-polarization during mid- and late-summer at large incidence angles were not made because of the sensitivity reduction.

8.3 Recommendations

Several radar backscatter measurements must be conducted in conjunction with adequate surface observations to supplement the existing data base and to answer the questions raised during this experiment. In addition to the backscatter data, the following experiments and suggestions should be considered to improve the data collection process.

(1) Dielectric constant measurements are needed for wet snow and ice at temperatures greater than -1° C at high frequencies, since there is very little published data.

(2) The ground truth should include some quantitative measurements of the wetness. During summer, even when the temperatures are below freezing, the snow melts because 10% - 30% of the solar radiation is absorbed by the upper layers of snow. This causes the snow to be warmed to temperatures near the melting point and, thus, the presence of wetness in the snow. This wetness increases the losses. There are two methods available to measure wetness in the snow: (1) the capacitance method and (2) the calorimeter method. The capacitance method is not as accurate as the calorimeter method, but the calorimeter method is time-consuming. Using the capacitance method to measure the snow wetness during future experiments should be investigated.

(3) It would be better to make measurements at an interval of 5° for incidence angles near vertical (less than 30°) and incidence angles greater than 60°. The measurements at incidence angles between 30° and 60° can be made at an interval of 15°.

(4) It is generally difficult to measure the imaginary part of the dielectric constant of the wet snow. A broad-band FM-CW radar should be used to determine the effect of snow cover and depth of penetration during summer. The HELOSCAT III was used to probe FYI during this experiment. This data is being analyzed and the preliminary results indicate that it

may be possible to infer the loss through the snow. The application of broadband FM-CW radar to determine the depth of snow was reported by Ellerbruch et al. [1978]. Therefore, a broadband FM-CW radar may be useful for determining the snow depth, the quantitative effect of snow cover on sea ice and layering in the snow and ice. A separate broadband FM-CW radar optimized for probing purposes should be developed. Personnel to operate this system continuously during the experiment should be provided.

(5) One site containing both FYI and MYI should be observed continuously to assess the full potential of radar in monitoring sea ice during the summer. The experiment should start in the early part of May and be continued into August or September.

TABLE 4
On the Ground

Angle = 60

	POWER RETURNS			MIN. MEAS. σ^o		
Freq	VV	HH	HV	VV	HH	HV
4.4	-29.00	-33.00	-41.00	-31.09	-42.26	-46.64
4.8	-31.00	-33.00	-44.00	-32.67	-40.40	-48.44
5.2	-34.00	-31.00	-47.00	-34.68	-38.31	-50.94
5.6	-34.00	-31.00	-49.00	-35.72	-39.05	-53.39
6.0	-34.00	-31.00	-52.00	-34.69	-37.57	-55.58
6.4	-35.00	-31.00	-53.00	-34.72	-36.05	-55.52
6.8	35.00	32.00	53.00	33.27	-35.81	53.97
7.2	-36.00	-33.00	-53.00	-33.53	-36.18	-53.35
7.6	-37.00	-33.00	-53.00	-33.57	-36.92	-53.35
8.6	-37.00	-33.00	-53.00	-33.57	-36.92	-53.25
8.6	-37.00	-31.00	-54.00	-25.93	-25.78	-46.01
9.6	-39.00	-33.00	-54.00	-19.06	-26.99	-43.27
10.6	-41.00	-39.00	-57.00	-24.38	=30.26	-44.31
11.6	-42.00	-41.00	-55.00	-16.99	-31.54	-37.81
12.6	-42.00	-42.00	-55.00	-17.94	-29.76	-36.99
13.6	-41.00	-40.00	-54.00	-18.04	-27.00	-36.11
14.6	-42.00	-39.00	-53.00	-16.50	-24.99	-33.05
15.6	-44.00	-43.00	-57.00	-13.76	-22.44	-31.55
16.6	-37.00	-32.00	-57.00	-6.35	-10.42	-30.52

TABLE 5
From Helicopter

ANGLE = 60

	POWER RETURNS			MIN. MEAS σ^o		
FREQ	VV	HH	HV	VV	HH	HV
4.4	-25.50	-29.00	-31.00	-27.59	-38.26	-26.64
4.8	-29.30	-28.00	-31.00	-30.97	-35.40	-35.44
5.2	-29.80	-25.00	-32.00	-30.48	-32.31	-35.94
5.6	-28.90	-24.00	-32.00	-30.62	-32.05	-36.39
6.0	-28.50	-24.00	-32.00	-29.19	-30.57	-35.58
6.4	-29.50	-25.00	-32.00	-29.22	-30.05	-34.52
6.8	-29.04	-23.00	-32.00	-27.31	-26.81	-32.94
7.2	-29.50	-23.60	-32.00	-27.03	-26.78	-32.35
7.6	-30.00	-26.80	-32.00	-26.57	-30.72	-32.25
8.6	-33.00	-32.00	-32.00	-21.93	-26.78	-24.01
9.6	-33.00	-32.00	-32.00	-13.06	-25.99	-21.27
10.6	-33.00	-32.00	-32.00	-16.38	-23.26	-19.31
11.6	-33.00	-32.00	-32.00	-7.99	-22.54	-14.81
12.6	-33.00	-32.00	-32.00	-8.94	-19.76	-13.99
13.6	-33.00	-32.00	-32.00	-10.04	-19.00	-14.11
14.6	-33.00	-32.00	-32.00	-7.50	-17.99	-12.05
15.6	-33.00	-31.00	-32.00	-2.76	-10.44	-6.55
16.6	-33.00	-31.00	-32.00	-2.35	-9.42	-5.52

NOTE: Altitude was assumed to be 50 feet and 3 dB was added to the power returns to calculate the minimum measurable σ^o with signal-to-noise ratio of 3 dB.

REFERENCES

Digby, S., "1982 Summer Ice Study: Experiment Summary and Ice Characterization Measurements," RadarSat/FIREX Program, November 1982.

Ellerbruch, D.A., et al., "Electromagnetic Scattering Properties of Soils and Snow," Proceedings of 12th International Symposium on RemoteSensing of Environment, April 20-26, 1978, pp. 957-974.

Gloersen, P., et al., "Microwave Signatures of First and Multiyear Sea Ice," JGR, vol. 70, no. 18, June 1983, pp. 3564-3572.

Gogineni, S.P., et al., "Mobile Microwave Spectrometer for Backscatter Measurements," accepted for publication in Microwaves and RF, September 1984.

Gray, A.L., et al., "Simultaneous Scatterometer and Radiometer Measurements of Sea Ice Microwave Signatures," IEEE J Oceanic Engineering, vol. OE-7, no. 1, January 1982, pp. 20-32.

Jacobs, J.D., et al., "Fast Ice Characteristics, with Special Reference to the Eastern Canadian Arctic," Polar Record, vol. 17, no. 110, 1975, pp. 521-536.

Livingstone, C.E., et al., "Classification of Beaufort Sea Ice Using Active and Passive Microwave Sensors," Proceedings of the Final SURSAT Ice Workshop, Toronto, Canada, June 23-27, 1980, Section 5.5.

Luther, C., et al., "Synthetic Aperture Radar Studies of Sea Ice," Proceedings of IGARSS'82, vol. II, Section TA 8, pp. 1.1 - 1.9.

Onstott, R.G., et al., "Four Years of Low Altitude Sea Ice Broadband Backscatter Measurement," IEEE J Oceanic Engineering

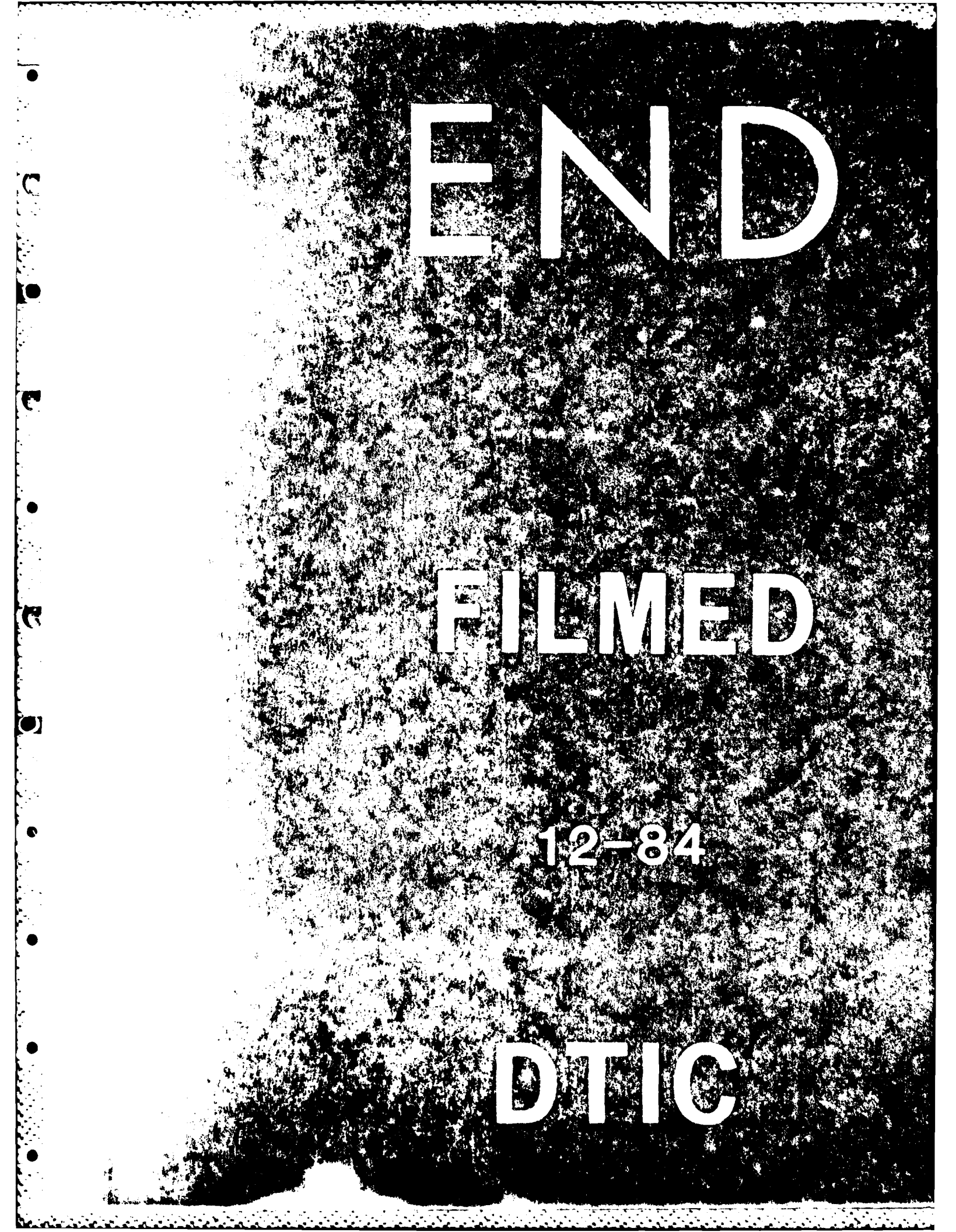
END
FILMED
12-84
DTIC